NREL/TP-451-21233 • UC Category: 1260 • DE96007892

High-Efficiency Thin-Film Cadmium Telluride Photovoltaic Cells

Annual Subcontract Report, January 20, 1995 - January 19, 1996

A.D. Compaan, R.G. Bohn, and
G. Contreras-Puente
Department of Physics and Astronomy
University of Toledo
Toledo, Ohio

NREL technical monitor: B. von Roedern

National Renewable Energy Laboratory
1617 Cole Boulevard
Golden, Colorado 80401-3393
A national laboratory of
the U.S. Department of Energy
Managed by Midwest Research Institute
for the U.S. Department of Energy
under Contract No. DE-AC36-83CH10093

Prepared under Subcontract No. ZAX-4-14013-1

May 1996

NOTICE

Available to DOE and DOE contractors from:
Office of Scientific and Technical Information (OSTI)
P.O. Box 62
Oak Ridge, TN 37831
Prices available by calling (423) 576-8401

Available to the public from:
National Technical Information Service (NTIS)
U.S. Department of Commerce
5285 Port Royal Road
Springfield, VA 22161
(703) 487-4650

SUMMARY

The University of Toledo photovoltaics group has been instrumental in developing rf sputtering for CdS/CdTe thin-film solar cells. During the second phase of the present contract our effort focussed on further optimizing the process of radio-frequency (rf) sputtering for the deposition of both the CdS layer and the CdTe layer to produce "all-sputtered" thin-film CdTe solar cells on glass. During the past year we began using an unbalanced planar magnetron for the CdS layer as well as for the CdTe layer in our two-gun sputtering chamber. We modified slightly some of the process parameters, including the contacting scheme, and raised the NREL-verified AM 1.5 cell efficiencies from 10.4% to 11.6% for cells fabricated on 10Ω/□ LOF soda-lime glass. This constitutes a new world record efficiency for an all-sputtered solar cell.

We participated in the CdTe Thin Film Teaming project with studies of thin CdS. For this effort we prepared cells on both 7059 borosilicate glass with conducting tin oxide layers deposited at the U. of South Florida and on LOF soda-lime glass with their textured SnO_2:F. Four types of cells were fabricated with CdS thicknesses of 300, 200, 100, and 60 nm. For each CdS thickness, cells on the 7059 and soda lime superstrates were prepared side-by-side through all steps in the preparation to facilitate direct comparisons. The 7059/USF SnO_2 superstrates had much better performance for CdS thicknesses below 200 nm..

Pulsed laser physical vapor deposition (LPVD) continues to be used for exploratory work on CdTe-related materials, especially where alloying or doping are involved and for the deposition of cadmium chloride layers. In order to study the properties of the critical interface region between the CdS and CdTe, we used LPVD to prepare alloy films of CdS_xTe_{1-x} on borosilicate glass and thin bilayer films of CdTe/CdS on fused silica. The composition of the alloy films has been determined by wavelength dispersive x-ray spectroscopy and other characteristics were measured by x-ray diffraction, Raman scattering, and optical absorption. Interdiffusion in the CdTe/CdS bilayers was measured by Rutherford backscattering and by photoluminescence.

Other characterization measurements in use at UT include Hall effect, electrical conductivity, current-voltage (I-V), spectral quantum efficiency (SQE), and frequency-dependent capacitance-voltage (C-V) measurements.

TABLE OF CONTENTS

LIST OF FIGURES

LIST OF TABLES

1.0 Introduction

1.1 Background

This annual report covers the second year of a three-year NREL subcontract with the University of Toledo which is focussed on improvements in efficiency for rf sputtered CdS/CdTe solar cells. In earlier work supported by NREL, the University of Toledo established the viability of two new deposition methods for CdS/CdTe solar cells by fabricating cells with above 10% AM 1.5 efficiencies on soda lime glass for "all-sputtered" cells and also for "all-laser-deposited" cells.[1,2] Recently, most of our effort has been placed on radio frequency sputtering (RFS) since it was judged to be more economical and more easily scaled to large-area deposition.[2,3] However, laser physical vapor deposition (LPVD) has remained our method of choice for the deposition of $CdCl_2$ layers and also for the exploration of new materials such as the ternary alloys including CdS_xTe_{1-x} and dopants such as Cu in ZnTe.

1.2 Technical Approach

RF sputtering--The process of rf sputtering admits of a considerable amount of flexibility in the deposition of CdS and CdTe. It is believed that the presence of significant densities of electrons, excited atoms and ions can be manipulated to improve the quality of the as-deposited films and/or lower the growth temperature due to the impact of energetic species on the film growth interface.[4] Much of our effort is designed to examine these effects with the ultimate goal of fabricating rf sputtered CdS/CdTe thin film solar cells with efficiencies exceeding 15% on soda-lime glass. In order to do this, it is important to obtain a thorough understanding of the fundamental science of the sputter-deposition process. We utilize a specially designed two-gun magnetron sputtering chamber with optical thickness monitors as described previously.[3] This chamber was originally equipped with two two-inch magnetrons one with a balanced magnetic field and the other with an unbalanced field. Because our early studies[3,5] showed that the unbalanced magnetron produced higher film quality, early this year we replaced the balanced magnetron with an unbalanced magnetron so that both CdS and CdTe depositions are now performed with two-inch diameter unbalanced magnetrons.

This year, in addition, we improved the rf matching network systems to reduce residual loss, carefully calibrated the power flow into the sputtering guns, and implemented a switching system to simplify the use of a single rf power supply for the two guns.

$CdCl_2$ treatment and contacting--We have continued the use of laser physical vapor deposition (LPVD) for the $CdCl_2$ application followed by the usual anneal at ~400C in air. For much of the past year we have continued to use evaporated Cu/Au contacts diffused at 150C, although these contacts are not very stable. However, near the end of this phase we collaborated with IEC for cell contacting. Subsequently we have revised our contacting scheme, following the IEC procedure of Cu deposition/anneal/Br-methanol etch/metallization. In our case, for convenience, we have evaporated gold as the final metallization. This has resulted in some improvement in stability of the cells and

more uniform response across the 2.5 inch square films.

Materials characterization/device testing--We continue to make extensive use of x-ray diffraction, Raman scattering, photoluminescence (PL), optical absorption, scanning tunnelling microscopy, and scanning electron microscopy with energy dispersive x-ray spectroscopy for studies of film morphology, structure, composition, and defects. We used four-point probe and van der Pauw measurements of conductivity as well as Hall effect measurements of carrier concentration and mobility. All fabricated devices are tested by current-voltage measurements, and some are tested for spectral quantum efficiency and by frequency-dependent capacitance-voltage measurements.

Exploratory work--In addition to the studies of standard CdS and CdTe materials, during the past year we have begun studies of the ternary alloy semiconductor CdS_xTe_{1-x} using LPVD for the film growth and Raman, PL, x-ray, and electrical measurements for the film quality. Alice Mason at NREL provided measurements of final film composition by wavelength dispersive x-ray spectroscopy. In order to examine interdiffusion across the CdS/CdTe interface we have fabricated by LPVD thin bilayers of CdTe/CdS/fused silica. This structure facilitates studies by Rutherford backscattering which is being done in collaboration with the Ion Beam Analysis Facility at Case Western Reserve University.

Finally, a considerable effort was placed on improving the reproducibility of the entire cell fabrication process involving rf sputtering, laser deposition, $CdCl_2$ treatment, annealing, contact application, and diffusion. We now are able regularly to produce films with an array of 4mm diameter cells in which all 36 cells have efficiencies in the range from 10.5 to 12%

2.0 Advances in Film Deposition and Cell Fabrication

2.1 Modifications to the sputter deposition facility

2.1.1 On-line quadrupole mass spectrometer

During the past year we have installed an on-line quadrupole mass spectrometer (Fisons VG). This has been used to monitor the base vacuum conditions in the sputter chamber. A top view sketch of the system showing the position of the mass spectrometer is given in Fig. 2.1. Note the two opposing magnetrons, the electrically floating rotatable heater/sample holder assembly, and the QMS sampling port for either base vacuum analysis or process gas and sputtered species analysis.

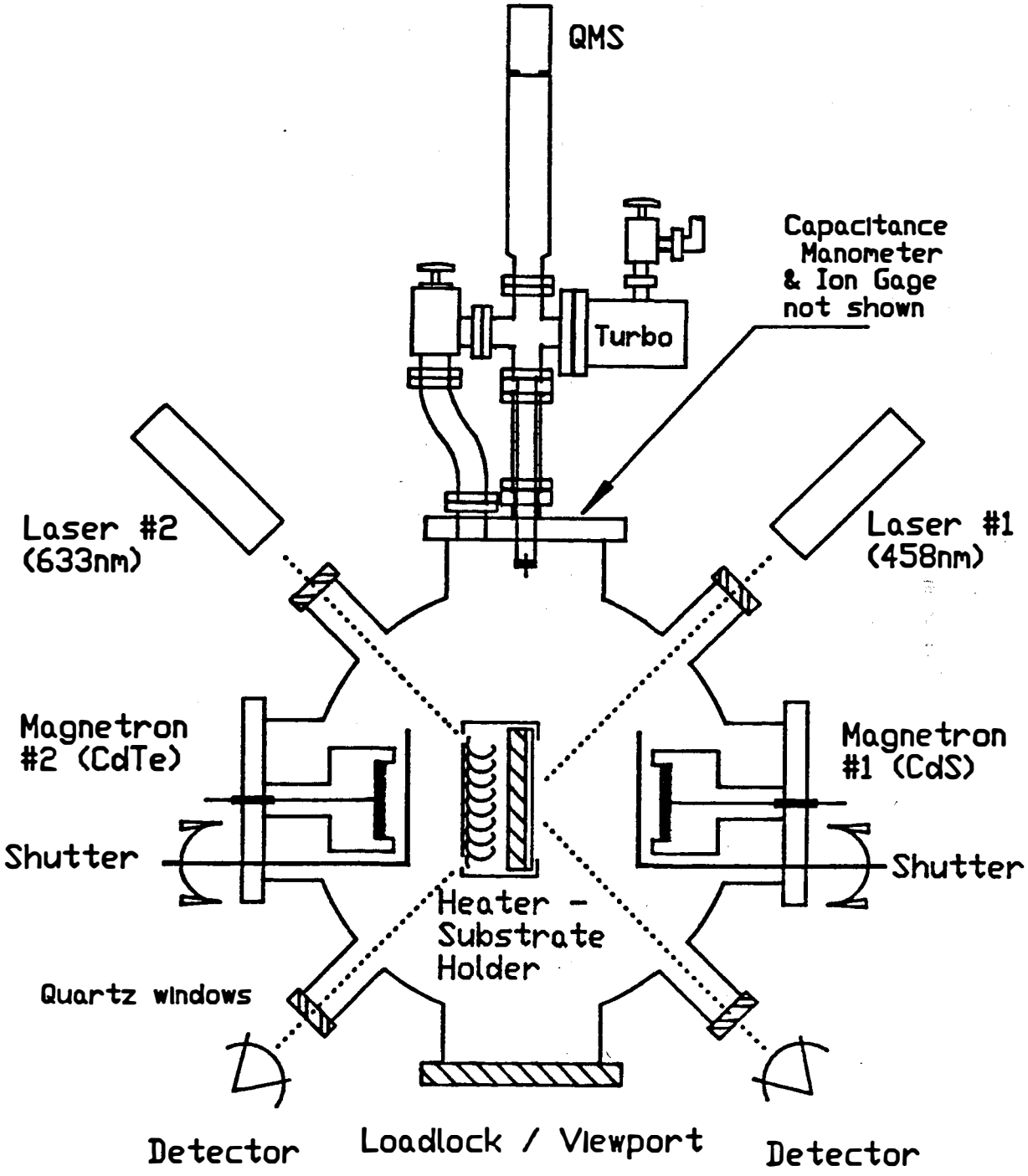

Fig. 2.1: Top view sketch of two-magnetron sputtering chamber showing rotatable substrate heater/holder, optical access ports, and quadrupole mass spectrometer.

An example of base vacuum analysis is given in Fig. 2.2, which shows the residual gases the residual gases during substrate heating at 380 C. Small quantities of common residual species such as H, H_2, H_2O, N_2, O_2, CO, CO_2, Ar and Fe are easily observed. The QMS system is presently connected directly to the chamber without additional pumping but differential pumping is being installed (See Fig. 2.1.) to permit sampling of process gases during the sputtering process which occurs at 10 to 50 mTorr. This should enable still tighter process monitoring and control.

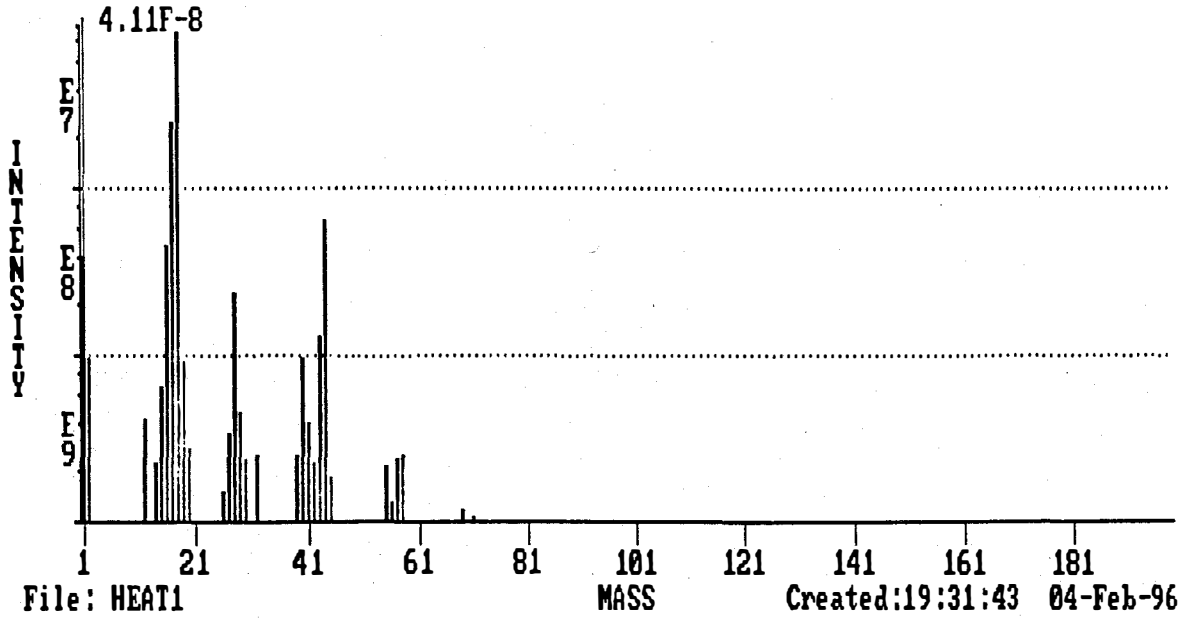

Fig. 2.2: Residual gas spectra from rf sputtering chamber a) with cold chamber, and b) with substrate heater on.

2.1.2 Unbalanced magnetron sputtering for both CdS and CdTe

In studies of film characteristics and cell performance during the previous contract year, we found that sputtering with an unbalanced magnetron yielded better film quality than sputtering with a balanced magnetron.[3,5] Therefore, early in this contract year we acquired a second two-inch diameter, unbalanced magnetron sputter gun from AJA International and replaced the balanced magnetron which we had been using for the CdS sputter growth. During the previous contract years we had used either a single, unbalanced gun for both CdS and CdTe films or, more recently, we had used the balanced gun for CdS deposition and the unbalanced magnetron for the CdTe layer. (Film quality of the CdS layer appears to be less critical to the photovoltaic performance--no doubt because most light is absorbed in the CdTe layer.) The use, this year, of unbalanced guns for both depositions contributed to some increase in cell performance. As discussed in the last annual report,[3] this

improvement in film quality appears to be due to the greater fluence of ions at the growth interface when the unbalanced gun is used. Direct tests of the influence of magnetron magnetic fields on the PV device performance are described in Section 2.3 below.

2.1.3 Changes in rf coupling into the magnetrons

Near the middle of this contract year we constructed a second rf matching network to avoid having to move the single matchbox from one magnetron to the other. In addition we implemented rf-compatible reed relays to be able to switch the rf power from one matching network/gun to the other. In the process, we replaced in the original matchbox an inductance element which was quite lossy. In order to correlate new measurements with work done using the old matching network, we measured the power coupled into the sputtering guns with old and new networks. Rf current was measured using a ferrite coil around the current lead to the sputter gun cathode. The ferrite pick-up coil was calibrated with a 50 Ω thin-film resistor load. The new matching network boxes have negligible loss. Earlier sputtering rate measurements must be adjusted to correct for the actual sputtering power input to the magnetrons. Some corrected measurements are discussed below.

Figure 2.3 shows the power transfer curve for the old matching network. Note that, due to resistive heating of the original inductor, the power coupled into the magnetron with the original matching network was highly nonlinear with respect to the power input to the matching network. In fact at the typical powers previously used (100 to 300 W) the actual power delivered to the gun ranged from ~20% to ~10% of the power delivered into the matching network.

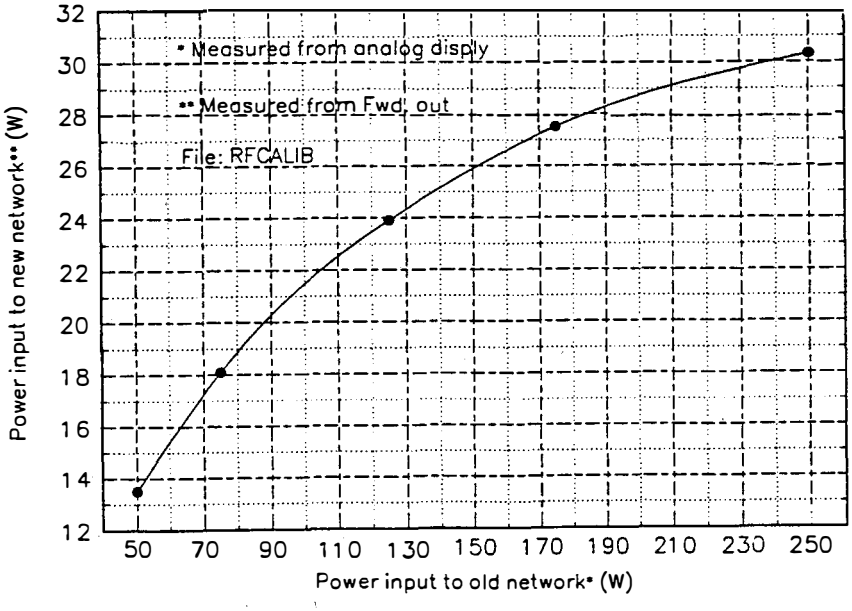

Fig. 2.3: Power transfer curve for the old rf matching network. (Since the new network has essentially zero loss, this calibrates the new system to the old system.)

Using this calibration of actual magnetron power vs. power delivered to the matching network, we show in Figure 2.4 a replot of a figure from our Annual Report for 1993 which shows growth rate of CdTe films on glass vs. rf power.[2] The corrected rate now shows little tendency to saturate with increasing rf power, at least up to 32 Watts. We have not attempted to determine growth rates at higher powers since we are using an unbacked sputtering target which is simply mechanically clamped to the cathode of the gun. No thermal conductive pastes or solders are used. This maximum power corresponds to 1.6 W/cm^2 averaged over our 5 cm diameter targets.

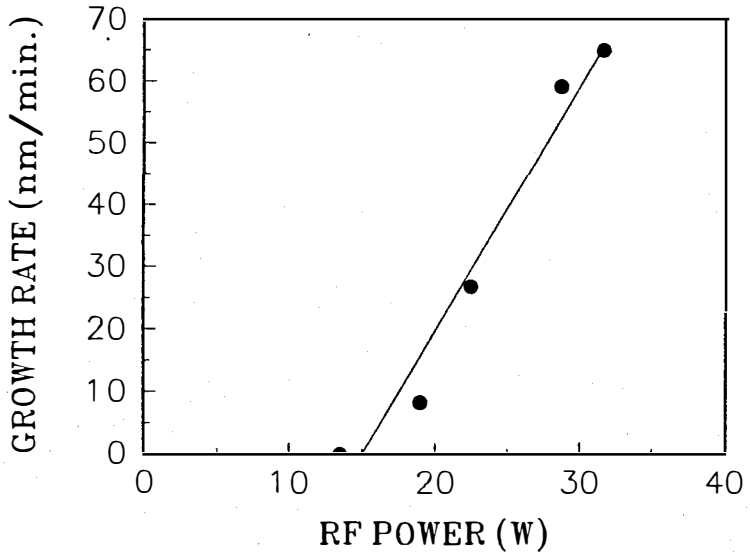

Fig. 2.4: Growth rate of CdTe at T_s= 310 °C vs. rf power for unbalanced magnetron. (Data replotted from Fig. 2-5a of ref. 2 using data of Fig. 2.3 above.)

2.2 *In situ* diagnostics for rf sputtering

2.2.1 Optical probes of substrate temperature and film thickness

As shown in Fig. 2.1, the present chamber is designed with four small windows at 45° to the film plane.[3] We regularly use these access windows to monitor, *in situ*, the film growth and also occasionally check the substrate glass temperature.[6] These measurements are done with the 633 nm line of a HeNe laser, for substrate temperature and the CdTe thickness, and the 458 nm line of an argon laser for the CdS film thickness. Details have been given in our Annual Report for 1994.[3]

2.2.2 Optical emission from the sputtering plasma

Rf sputtering is characterized by large quantities of excited state species, originating both from the sputtering gas (Ar) and from species sputtered from the target (e.g., Cd). Copious amounts of light are emitted from these excited species and this light is useful as a diagnostic.[7] Our objective is, not only to improve our understanding of the process, but also to identify sensitive and convenient methods for process control during deposition. Spectra were obtained by imaging the plasma through the load door window into a fiber optic bundle with spot and slit end configurations. The fiber bundle end with the slit geometry was proximity imaged into the entrance slit of a 1/4 meter spectrograph

(Aries FF250) equipped with a PAR OMA-II vidicon. Examples of two spectra, taken from the Ph.D. thesis of Meilun Shao,[7] are shown in Fig. 2.5a and 2.5b. One may clearly observe emission lines corresponding to neutral Ar (ArI), singly ionized Ar (ArII) and neutral Cd (CdI) and ionized Cd (CdII). The atomic state origins of these emission lines are given in Table 2.1.

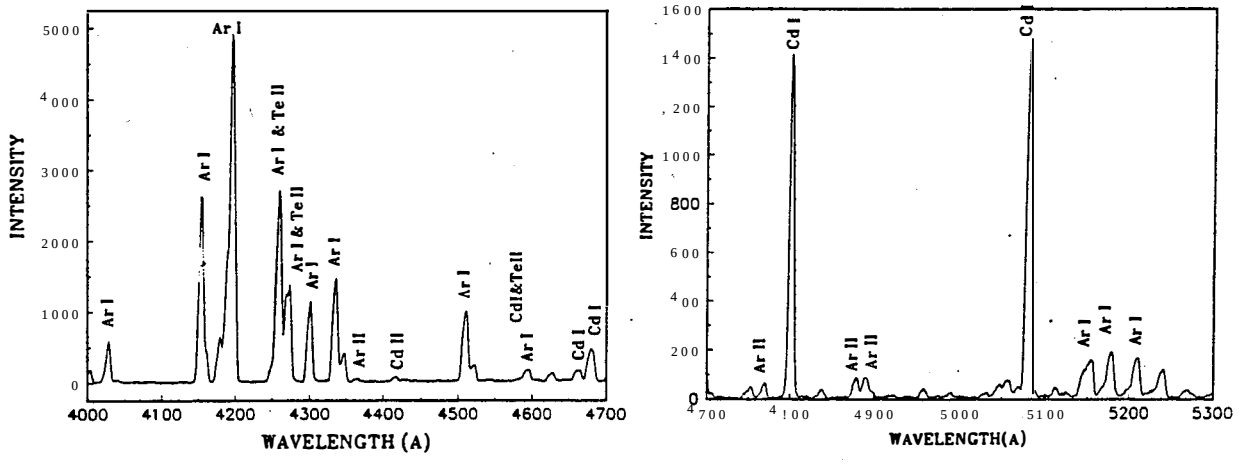

Fig. 2.5: Spectra observed during rf sputtering of CdTe. Observed 4mm from target cathode with P_{rf}= 26 W, p_{Ar}=18 mTorr. (From ref. 7.)

Table 2.1: Atomic transitions observed in rf sputtering plasma with CdTe target

SPECIE	λ (nm)	UPPER STATE	LOWER STATE
ArI (neutral)	518.8	$3p^5 5d$ (15.30 eV)	$3p^5 4p$ (12.91 eV)
ArII (ion)	488.0	$3p^4 4p\ ^2D_{5/2}$ (35.43 eV)	$3p^4 4p\ ^2P_{3/2}$ (32.89 eV)
CdI (neutral)	508.6	$4d^{10} 5s6s\ ^3S_1$ (6.38 eV)	$4d^{10} 5s5p\ ^3P_2$ (3.95 eV)
CdII (ion)	441.6	$4d^{10} 5d\ ^2D_{5/2}$ (17.5 eV)	$4d^{10} 5p\ ^2P_{3/2}$ (14.8 eV)

Three representative emission lines are shown in Fig.2.6 as a function of rf power coupled into the unbalanced magnetron. A region approximately 4mm above the surface of the sputtering target was imaged into the fiber end. This distance is slightly beyond the region of maximum brightness above the magnetron track.

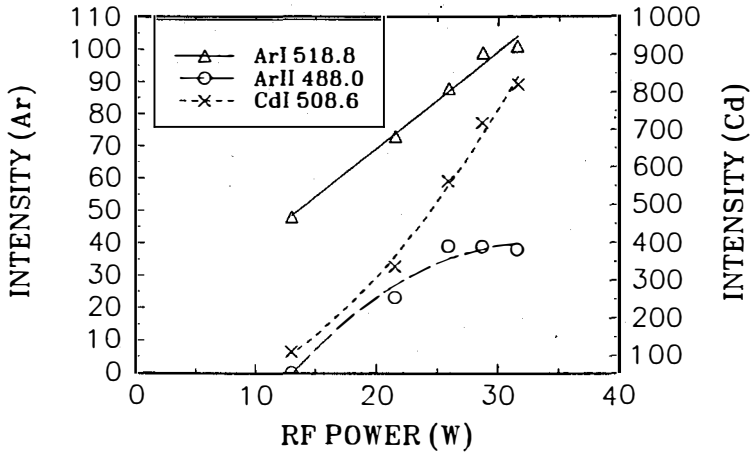

Fig. 2.6: Light emission 4 mm above cathode vs. rf power for a) ArI (518.8 nm), b) ArII (488.0 nm), and c) CdI (508.6 nm). (From ref. 7.)

Some light emission extends even to the substrate, a distance of 7 cm from the 5 cm diameter sputtering target. Fig. 2.7 shows the intensity of this light emission from excited state Cd atoms as a function of the rf power into the magnetron. For these data the Cd line intensity was normalized to the intensity of the neutral argon at 518.8 nm. For comparison, we have shown in Fig. 2.7 the CdTe film growth rate at T_s=310 C. Clearly, the Cd emission line at 508.6 nm tracks the film growth rate quite well for this geometry and this range of rf power. Most of our recent cell fabrication has been done at a rate of ~30 nm/min.

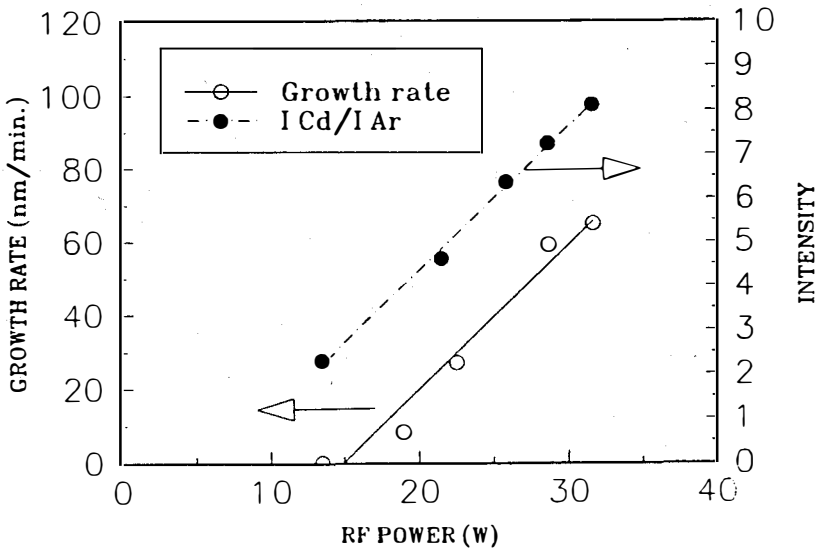

Fig. 2.7: Emission intensity of 508.6 nm CdI line near the substrate and CdTe growth rate vs. rf power.(From ref. 7.)

Some of the physics inherent in the magnetron deposition process is illustrated in the pressure dependence of the light emission intensities ~4 mm above the target for several species as shown in

Figs. 2.8 - 2.11, all taken from ref. 7. Figs. 2.8 and 2.9 show the emission intensities for neutral and ionized Ar vs. Ar gas pressure for three rf sputtering powers. Note that neutral Ar emission rises to 15 mT and then saturates but the emission from ionized Ar decreases from 2 mT even though the total Ar pressure is rising. This behavior is closely related to the lower excited state energy for neutral Ar (~15 eV) as compared with ionized Ar (~35 eV). For neutral Cd, shown in Fig. 2.10, the intensity increases almost linearly with Ar pressure over the range studied. However, the Cd ion line decreases with increasing Ar gas pressure, as shown in Fig. 2.11. The excited state energy for the neutral Cd line at 508.6 nm is unusually low (~6 eV) and is not strongly affected by Ar gas pressure but the 441.6 nm CdII line originating from a 17.5 eV state would be very sensitive to electron energies. The pressure dependence of these two ionic transitions gives qualitative indications of the relatively low electron energies in the sputtering plasma.

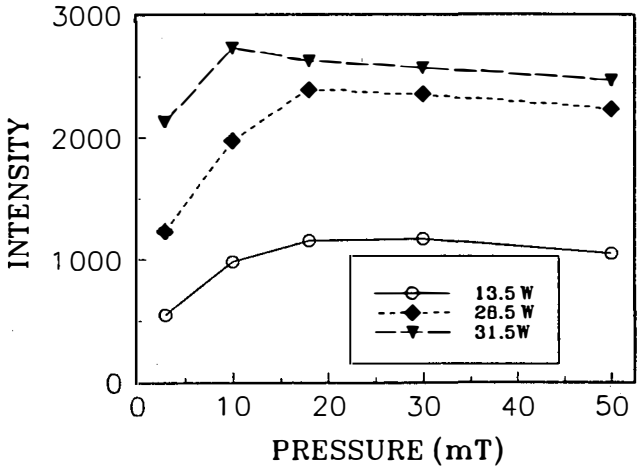

Fig. 2.8: Intensity of ArI (518.8 nm).

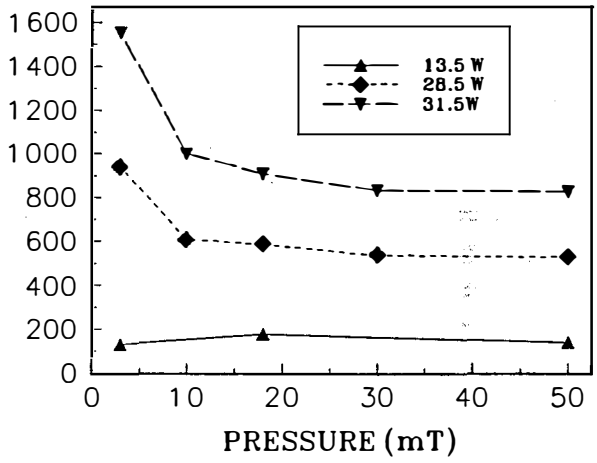

Fig. 2.9: Intensity of ArII (488.0 nm).

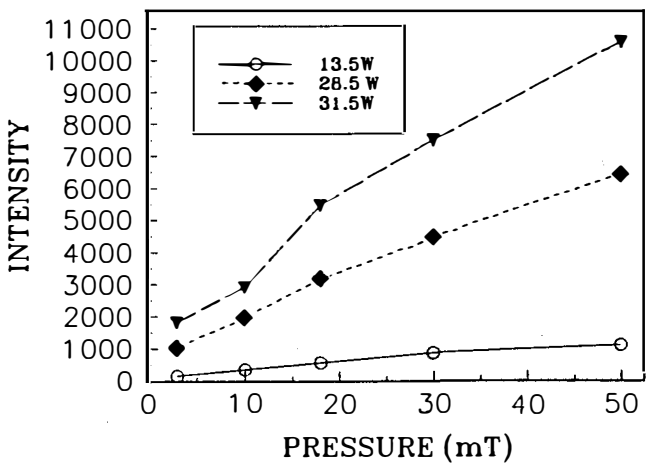

Fig. 2.10: Intensity of CdI (508.6 nm).

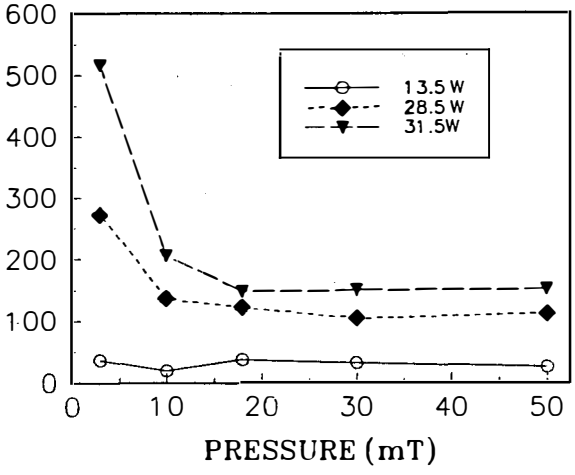

Fig. 2.11: Intensity of CdII (441.6 nm).

2.3 Cell performance dependence on magnetron magnetic field

We have reported previously on some of the changes in materials properties which arise from the magnetic fields of the planar magnetron sputtering guns.[3,5] We found that the film characteristics are improved when the unbalanced gun is used for deposition. In addition, we have described the effect on device performance of switching CdTe and CdS targets between balanced and unbalanced magnetrons. The device performance dropped from ~10%, when the unbalanced gun was used for CdTe deposition and the balanced gun for the CdS layer, to ~4% when the balanced gun was used for CdTe and the unbalanced gun for CdS, even though all other processing parameters were held fixed. The use of the unbalanced magnetron for deposition of the CdTe layer is important, presumably because long minority carrier lifetimes are critical in the absorber material CdTe and much less so in the window material CdS.

After acquiring a second unbalanced magnetron we have been able to perform a more direct analysis of the magnetic field effects. First we fabricated cells maintaining the unbalanced gun for CdTe deposition and used either another unbalanced gun or the balanced gun for the CdS layer. Then we made a similar test using the unbalanced magnetron for the CdS deposition and either the second unbalanced gun or the balanced gun for the CdTe deposition. To avoid possible influence from the slightly different diameter erosion tracks of the balanced and unbalanced guns, we used a fresh CdS target. (We have measured the diameter of the erosion tracks to be 2.5 cm for the unbalanced gun and 2.9 cm for the balanced gun.) The results of the cell performances are shown in Table 2.2. I-V curves of the best cells prepared from those films are shown in Fig. 2.12.

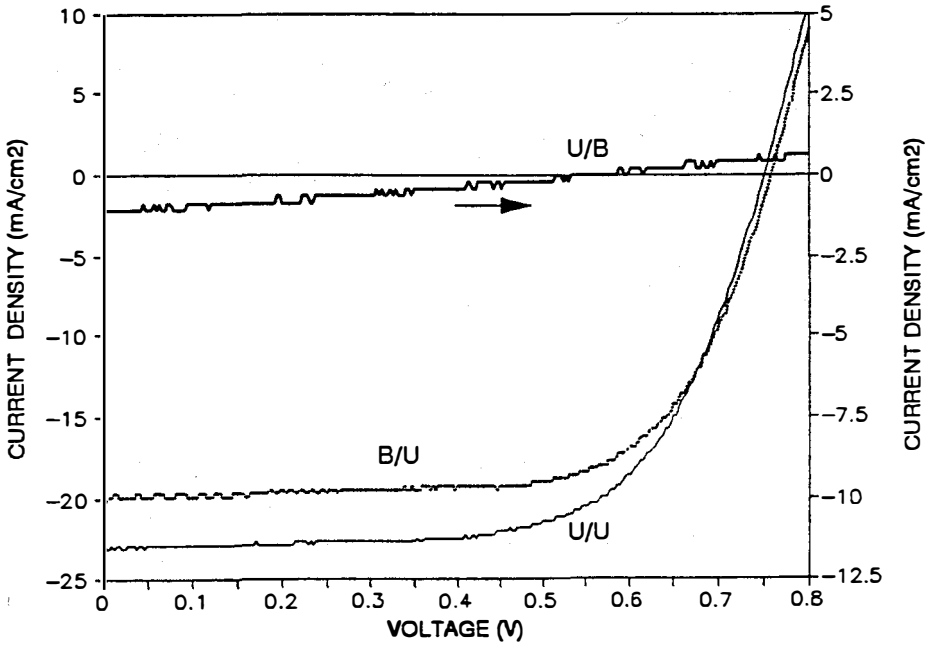

Fig. 2.12: Best cell performance for three variations of magnetron magnetic field structures for the CdS/CdTe depositions respectively: unbalanced/unbalanced (U/U), unbalanced/balanced (U/B), and balanced/unbalanced (B/U).

Table 2.2: Device performance with combinations of balanced and unbalanced magnetrons

CdS/CdTe depositions	V_{oc}(mV)	J_{sc}(mA/cm^2)	FF	η
unbalanced/unbalanced	751	22.9	66.3	11.4
balanced/unbalanced	758	20.1	67.8	10.3
unbalanced/balanced	516	1.5	40.5	0.23

2.4 Improvements in CdTe contacting

In order to focus on improvements in the CdS and CdTe layers and in the $CdCl_2$ treatment and annealing, we have been using a relatively simple contacting procedure involving sequential evaporation from adjacent boats of about 40 Å of Cu followed by 200 - 500 Å of gold. This structure was then diffused at 150 C for 30 minutes. This contact has proven to be quite reproducible but it is not stable. For example, a cell which begins at 11% efficiency decays to about 10% efficiency in about one week, whether or not it is under illumination. Recently the Institute for Energy Conversion contacted several cells on our rf sputtered films. (See discussion under Section 3.2.) These showed promising results, and we have recently begun using a similar method for contacting. Presently the variation on the IEC procedure which we use consists of 10 nm of copper evaporation followed by 160 C anneal in flowing Ar gas. A 20 - 30 second etch in 0.05% Br/methanol removes the excess copper. The structure is then placed into the evaporator again for the deposition of gold contacts. This procedure has improved the stability of the contacts and produced more uniform efficiency over the main part of the film area.

A side-by-side comparison of efficiencies and stabilities for cells prepared with the old contacting method, "method 1" (30Å Cu / 200Å Au /150 ^{o}C diffusion) with the IEC-based procedure, "method 2" (100Å Cu/160 C diffusion/etch/200Å Au) is shown in Fig. 2.13. These results are taken from two halves of the same film, i.e., all other process conditions were identical. These cells were prepared on 3mm thick 10 Ω/□ LOF soda-lime glass. Note that the best cell efficiencies are approximately 12% for each method, however, the stability is improved for the IEC-based procedure, even though the metals are the same.

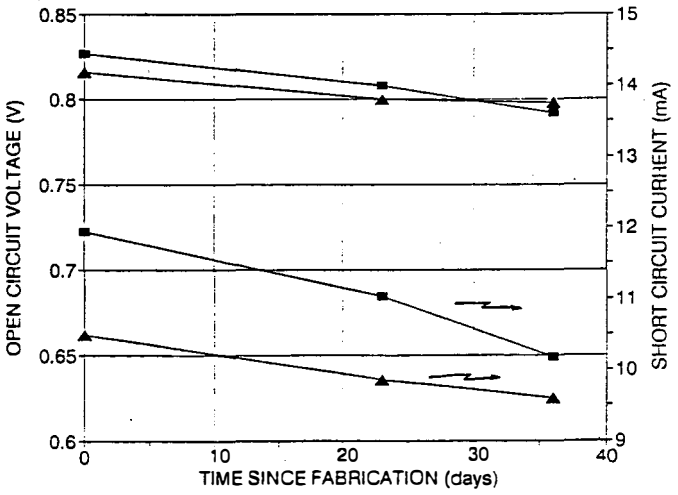

Fig. 2.13: Stability of cells contacted with ■ = method 1 (Cu+Au+diffusion) or ▲ = method 2 (Cu+diffusion+ etch + Au).

The data of Fig. 2.13 indicate that considerable instability can result from the contact method. Additionally we have tested for instability in the junction and absorber region by recontacting cells several months after the initial fabrication. Typically we use a grid of 4 mm dots on a 7 mm square pattern. Thus we can fabricate new contacts between the original contacts. For the 40Å Cu / 200Å Au / 150C diffusion method ("method 1"), the second set of contacts are entirely new. For the IEC-based method, 100Å Cu / 160C diffusion / Br-meth etch / 200Å Au ("method 2"), the original Cu evaporation covers the entire film area and only the Au evaporation is redone.

We find that films originally contacted with method 1 and then recontacted at adjacent spots with method 1 after 40 days had nearly identical performance of ~11% even though the original cells had deteriorated from ~11% to ~9.5% in efficiency. This indicates that, without the Cu and Au contact materials present, the semiconductor layers are stable. For the case of cells originally contacted with method 2, the performance deterioration was less, from ~11% to ~10%, but the evaporation of new gold contacts gave results which were no better than the original (deteriorated) contacts. This suggests that copper diffused into the CdTe is responsible for much of the instability even though in the case of method 2 there was an etching step after the Cu diffusion. Before a final indictment of the Cu diffusion method however, we cannot rule out the possibility that further adjustments to the etching process might improve the stability.

Additional information on contact stability is presented in Section 3.2 regarding contacts prepared at IEC on our sputtered films with graphite final contacts. These copper-diffused contacts finished with graphite appear to be quite stable, indicating that this method should be further investigated for use with sputtered CdTe cells.

2.5 NREL tests of recent "all-sputtered" cells

At the end of the Phase Two of this contract, we supplied several cells to NREL on superstrates of 10 Ω/□ LOF soda-lime glass. The cell structure was rf sputtered CdS 250 nm thick and rf sputtered CdTe 1.8 μm thick. Following the rf sputtering, we used our standard application of $CdCl_2$ by laser deposition and 15 minute anneal in air at 400 C followed by a deionized water rinse. However, no other treatment was given either to the CdS or the CdTe which were sputtered in the single chamber shown in Fig. 2.1. The contact structure was diffused and etched copper followed by 500 Å of evaporated gold--as described in Section 2.4 above. The test results supplied by Halden Field are shown in Figs.2.14 and 2.15.

These cells have limited current response in the blue because of the relatively thick CdS (250 nm), however, the voltage and fill factors are good. After testing at NREL, we remeasured the cell performance at UT with our tungsten lamp simulator and found that the performance had deteriorated by about 0.8% absolute between our first test immediately after fabrication and the retest four weeks later. Thus some improved performance should be realizable with better stability of the contacts. Aggressive efforts are underway to find stable contacts to the rf sputtered cells with at least equivalent performance. In addition, higher currents should be achievable with thinner CdS as is demonstrated in Section 3.1 below. In order to avoid loss of voltage and fill factor however,

thinner CdS may require a multilayer TCO, for example, the use of an intrinsic layer next to the CdS. The spectral quantum efficiency shown in Fig. 2.15 also shows that there is some loss of current in the red (700-850 nm), presumably due to deep penetration in the CdTe. This could be improved with thicker CdTe but may require a somewhat lower resistivity material. Further, an anti-reflection coating on the glass will yield some additional current. At this point we believe, from the results shown above, that rf sputtering of both the CdS and the CdTe layers should be capable of reaching and possibly exceeding 15% efficiencies.

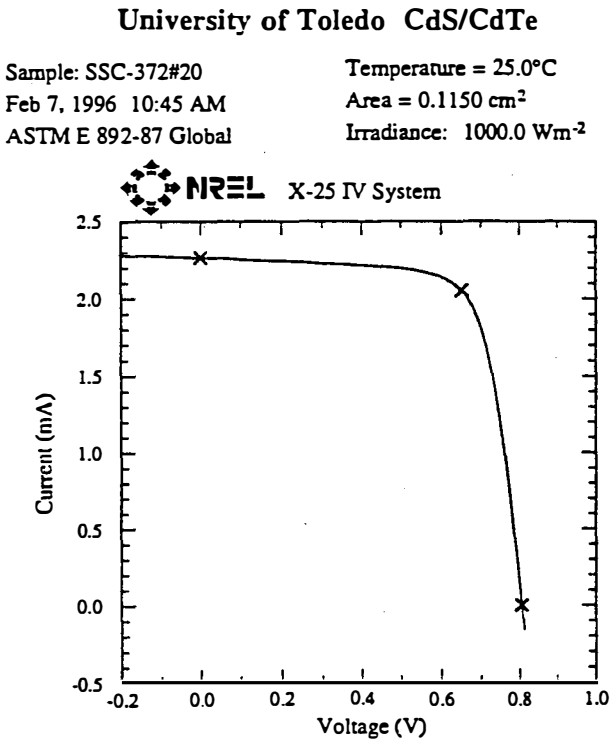

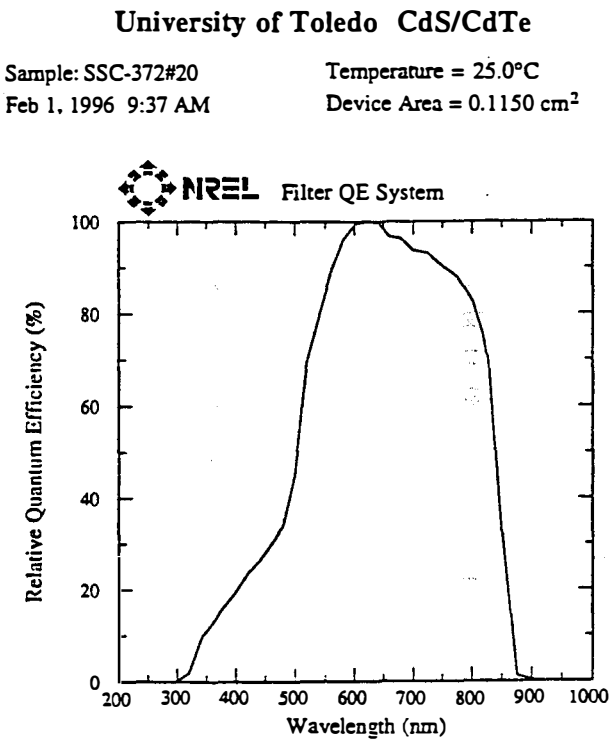

V_{oc} = 0.8056 V
I_{sc} = 2.266 mA
J_{sc} = 19.70 mAcm^{-2}
Fill Factor = 73.27 %

V_{max} = 0.6514 V
I_{max} = 2.053 mA
P_{max} = 1.337 mW
Efficiency = 11.6 %

10 min soak @ P_{max}, 6:13 cool, fast sweep, fan on

Light Bias = 2.000 mA
Bias Voltage = 0.00 V

J_{sc} = 22.59 mA/cm^2 for ASTM E 892 Global (1000 W/m^2)

Fig. 2.14: I-V response of all-sputtered cell SSC372, contact 20.

Fig. 2.15: Relative spectral quantum efficiency of cell SSC372, contact 20.

3.0 CdTe Thin Film Partnership Teaming Activities

3.1 Thin CdS Team

We participated in the "Thin CdS" team of the CdTe Thin Film Partnership activities by preparing "all-sputtered" CdS/CdTe cells on superstrates supplied by Chris Ferekides of the University of South Florida. These were 7059 Corning glass superstrates 0.8 mm thick and 1.25 x 1.5 inch. The doped SnO_2 layers were deposited by USF. Since our standard substrate size for rf sputtering is 3 inch by 2.75 inch, we fabricated a stainless steel jig to hold the smaller 7059 samples. This jig was constructed so that we could also mount a 1.25 x 1.5 inch piece of 10 Ω LOF glass. The 7059 substrate was slightly closer to the centerline of the sputtering guns and mounted so that our HeNe laser and Ar laser optical thickness monitors could pass through the Corning glass substrate. Other than the slight asymmetry in the sample holder, the 7059 and LOF superstrates were subjected to identical environments during the cell fabrication. A sketch of the sample jig is shown in Fig. 3.1. We have determined that the film thickness decreases to about 85% at a distance of 1.25 inches from the center of the deposition. Thus we expect that the CdS and CdTe films on the LOF glass are at most 10% less than those on the 7059 glass. We note that the thickness of the CdS and the CdTe on the LOF glass were not monitored *in situ*. Post-deposition optical absorption shows that the CdTe thickness on the LOF glass was within 10% of that on the 7059.

With the new stainless steel sample jig and Corning glass samples, we checked the substrate temperature using the optical interference method with the HeNe laser. All cell growths were performed at 380 C. Four different depositions were made with two small superstrates (7059 and LOF) for each run. CdS/CdTe sputtered layers were made with CdTe thickness of 1.8 μm and CdS thicknesses of 600 Å, 1000 Å, 2000 Å, and 3000 Å. The CdS and CdTe thicknesses were measured *in situ* but the various thicknesses correlated well with the growth time as well.

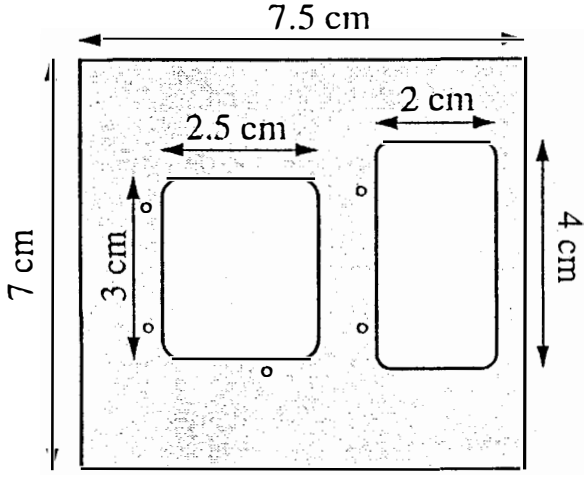

Fig. 3.1: Sample holder used for small 7059 and LOF glass superstrates.

After our standard processing, which includes the LPVD $CdCl_2$ deposition and 400 C anneal in air, Cu/Au 4 mm diameter circular contacts were evaporated and diffused at 150 C. (No etching was done.) As mentioned above, these diffused contacts are not stable and we monitored the performance of at least one cell on each film for a period of about two weeks before sending the cells to Colorado State University for testing. Our tests of cell performance during the first several days of cell life are shown in Figs. 3.2 - 3.5 which show the decay over several days of V_{oc}, J_{sc}, fill factor, and efficiency. Over about two weeks V_{oc}

decays by up to 2%, J_{sc} decays by 7 to 10%, fill factors by 4-6%, and efficiencies by 10 - 17%. Our measurements were done with an ELH lamp standardized to a Si reference cell and have an estimated absolute error of ±1% in efficiency (±10% relative error). Modeling the J-V curves indicates that the primary change with time is the apparent series resistance at AM 1.5. For the cell with 1000 Å CdS layer, the apparent series resistance increased from 3.6 Ω-cm^2 to 4.5 Ω-cm^2, whereas for the cell with 600 Å of CdS, the apparent series resistance increased from 4.0 Ω-cm^2 to 6.3 Ω-cm^2. We believe that the instability is wholly or, at least primarily, due to deterioration of the diffused Cu/Au contact (method 1, as discussed in Sec. 2.4).

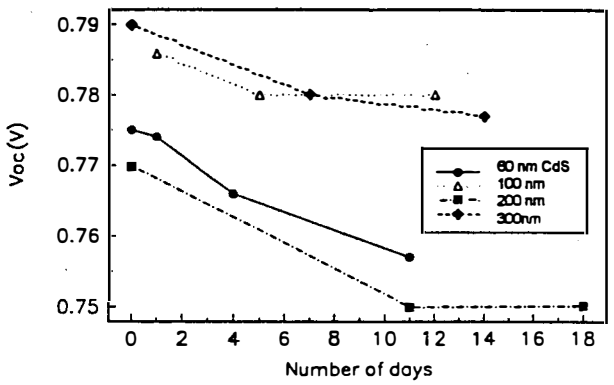

Fig. 3.2: Decay of V_{OC}.

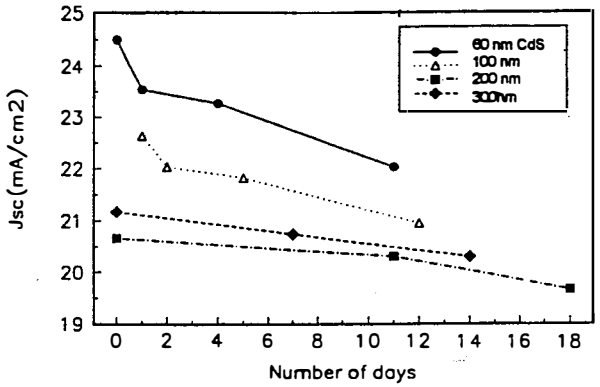

Fig. 3.3: Decay of J_{SC}.

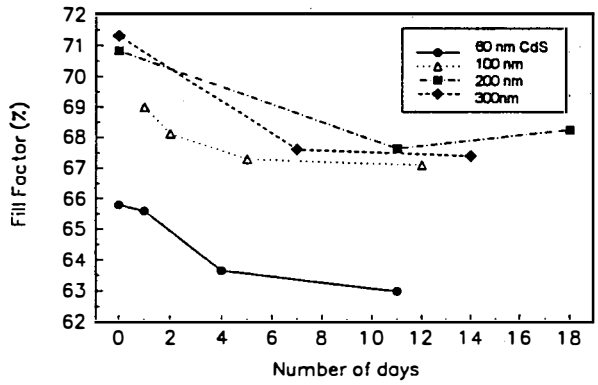

Fig. 3.4: Decay of fill factors.

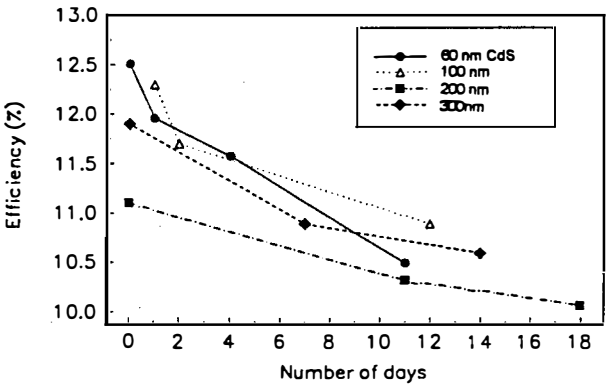

Fig. 3.5: Decay of cell efficiencies.

Detailed measurements and analyses of the cell performances were done at Colorado State by J. Granata and J. Sites. We supplied eight cells, four on the 7059/USF superstrates and four on the 10 Ω/□ LOF superstrates. Each of the superstrates had six 4 mm diameter cells defined. In two cases CSU analyzed the same contact as we had monitored--the cells with 600 Å and 1000 Å CdS thicknesses. A full set of results is provided in Tables 3.1 and 3.2. The CSU measurements of the efficiency of these cells are plotted also as the final points on Fig. 3.5. It is interesting to note that the efficiency reported by CSU was higher by almost 1 full percent than our last measured value.

Figures 3.6 and 3.7 give the light and dark I-V response of the eight cells with the four different CdS thicknesses. The forward current in the dark shows the effects of very high series resistance. Especially in the case of the cells on LOF glass, the light I-V curve shows considerable roll-over in the forward current case. Most of these effects are plausibly attributed to poor performance of the contacts.

Table 3.1: U.T. sputtered cells grown on U.S.F. SnO_2:F/ 7059 superstrates.

RUN	SSC303 14	SSC304 7	SSC305 14	SSC306 21
CdS [Å]	3000	2000	1000	600
Total area [cm^2]	0.113	0.113	0.113	0.113
V_{oc} [V]	0.79	0.78	0.78	0.76
J_{sc} [mA/cm^2]	19.6	19.6	22.4	24.2
V_{mp} [V]	0.65	0.61	0.60	0.57
J_{mp} [mA/cm^2]	16.7	16.7	19.5	20.2
FF	0.70	0.67	0.68	0.62
η%	10.8	10.2	11.9	11.4
r [Ω-cm^2] light/dark	1300 >10000	900 >10000	890 >10000	890 >10000
A light/dark	2.7 1.0	3.0 1.5	2.3 1.7	2.7 1.7
R[Ω-cm^2] light/dark	0.3 14	0.3 11	1.8 17	2.5 17
depletion layer thickness [μm]	2.0	1.7	1.9	2.1
hole density [cm^{-3}]	~10^{17}	~10^{17}	~10^{17}	~10^{17}

Table 3.2: U.T. sputtered cells grown on LOF SnO_2:F/ soda-lime glass superstrates.

RUN	SSC303 18	SSC304 12	SSC305 11	SSC306 17
CdS [Å]	3000	2000	1000	600
Total area [cm^2]	0.113	0.113	0.113	0.113
V_{oc} [V]	0.80	0.76	0.60	0.49
J_{sc} [mA/cm^2]	19.9	21.2	23.1	24.0
V_{mp} [V]	0.65	0.57	0.41	0.35
J_{mp} [mA/cm^2]	17.3	18.5	20.3	20.6
FF	0.71	0.65	0.60	0.60
η%	11.3	10.5	8.3	7.1
r [Ω-cm^2] light/dark	1100 >10000	890 >10000	920 >10000	830 >10000
A light/dark	2.3 1.6	2.7 1.1	1.6 1.9	1.5 ---
R[Ω-cm^2] light/dark	0.7 11	1.8 15	3.9 60	3.1 —
depletion layer thickness [μm]	1.9	1.6	1.9	2.0
hole density [cm^{-3}]	~10^{17}	~10^{17}	~10^{17}	~10^{17}

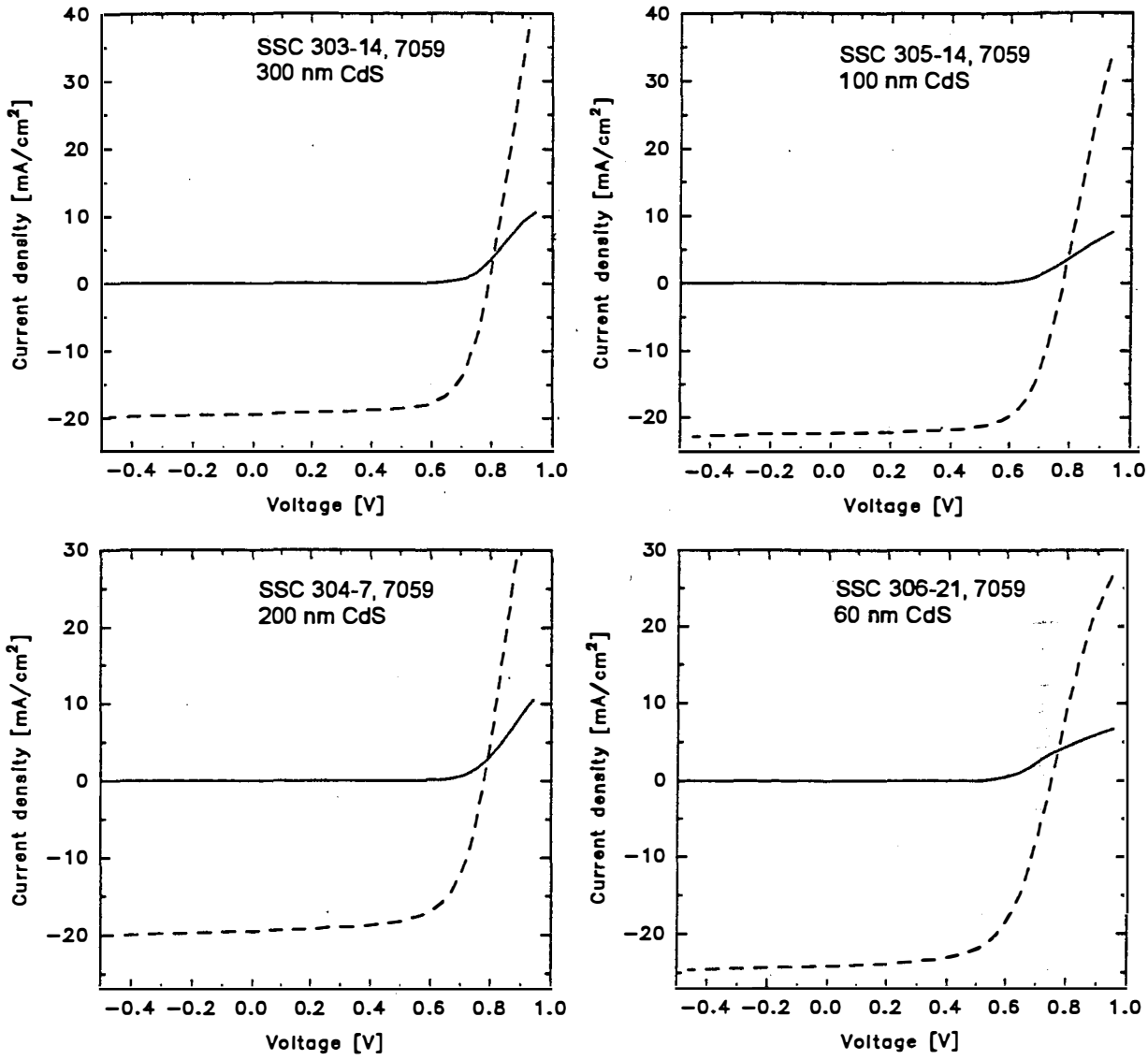

Fig. 3.6: One-sun light and dark I-V curves for sputtered cells on 7059/(USF SnO_2:F) glass with four different CdS thicknesses: 300, 200, 100 and 60 nm. Contacts by method 1. Results supplied by J. Granata and J. Sites.

Among the sets of CdS thicknesses supplied by five different groups for this teaming work, the UT cells covered the widest range of CdS thicknesses. The cell efficiencies at AM 1.5 fell in the middle of the range in this study. The UT group was the only group to supply cells on soda-lime glass as part of this study. It is interesting that for thick CdS (3000 and 2000 Å) our cells on soda-lime (LOF) glass outperformed our cells on the 7059 glass in spite of the fact that the 7059 glass is more transparent and the USF SnO_2 coating has less haze. We suggest that this may arise from the fact that our process has been optimized with the LOF glass.

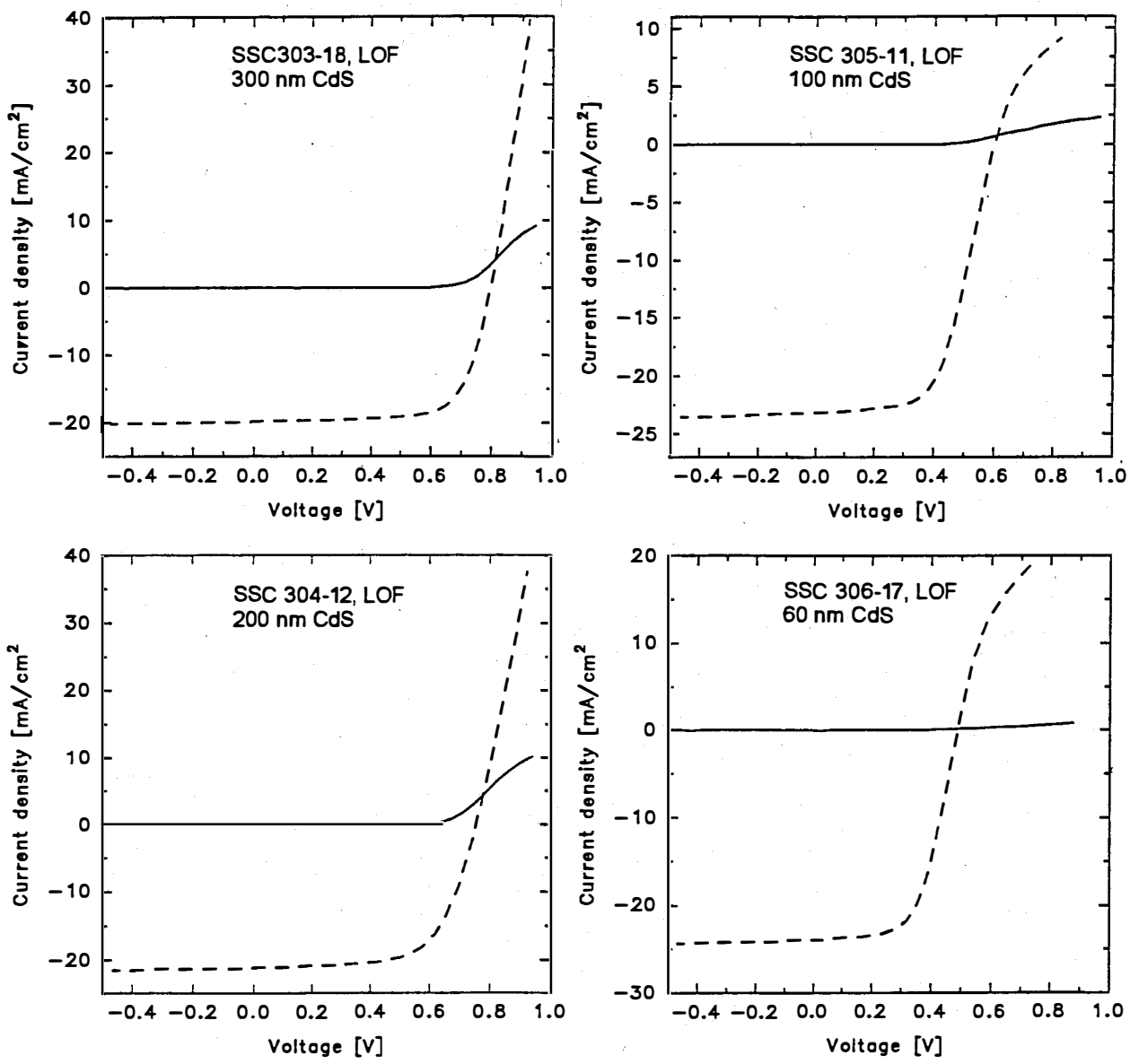

Fig. 3.7: One-sun light and dark I-V curves for sputtered cells on LOF 10 Ω/□ SnO_2:F glass with four different CdS thicknesses: 300, 200, 100 and 60 nm. Contacts by method 1. Results supplied by J. Granata and J. Sites.

3.2 Thin, sputtered CdS comparison--7059/USF vs. soda-lime/LOF

In spite of the performance deterioration which occurs with the diffused Cu/Au contacts which were used for this collaborative work, it is possible to make a direct comparison between the two types of substrates and their relative effects on the cell performance with thin CdS. In the data presented below, we utilize numbers we obtained immediately after the cell fabrication ended. That is, the testing was done within hours after cell completion. Note that these measurements were made with

an ELH tungsten-halogen lamp which we estimate to yield efficiencies within 0.5% of NREL-calibrations. This is based on experience with recent cell tests at NREL. (See Section 2.5 above.) However, it is quite likely that this lamp underestimates the current in cells with very thin CdS which have much better response in the blue (< 550 nm).

Cell comparisons are shown in Figs. 3.8 - 3.10, which give the V_{OC}, J_{SC}, and fill factors for one cell each on a 7059 superstrate and a soda-lime superstrate which were fabricated together. Fig. 3.8 shows that open circuit voltage is quite stable on the 7059 superstrates with USF-deposited TCO, however, on the LOF-10Ω/□, Cds thicknesses below 200 nm show increasing voltage loss. On the other hand, short circuit currents behave quite similarly with the two superstrates. Both show the expected increase in current as the CdS thickness decreases below 200 nm (The fact that the LOF substrate was mounted slightly away from the sputter gun axis and received slightly less CdS may explain the higher current for the 60 nm point. We estimate that the CdS thicknesses for the LOF superstrates were all about 10% less.) Both sets of superstrates show loss of fill factor as the CdS thickness decreases but the LOF superstrates showed more serious loss.

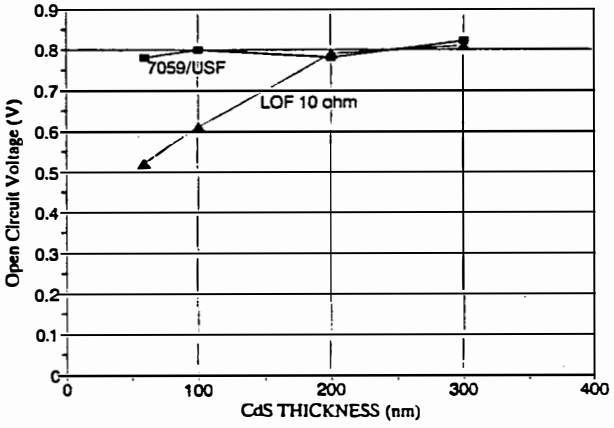

Fig. 3.8: V_{OC} for cells on 7059 and LOF glass, processed side-by-side.

Our conclusion is that the multilayer SnO_2 deposited by the University of South Florida is largely responsible for the differences seen in open circuit voltage and fill factors for the thin CdS cases. Presumably the resistive top layer and possibly the smoother texture of the USF TCO are responsible for these effects. It should be noted that our sputtering process has been optimized with LOF superstrates and the performances shown above and in Section 3.1 probably do not represent the best that can be achieved with an "all-rf-sputtered" cell on 7059 glass.

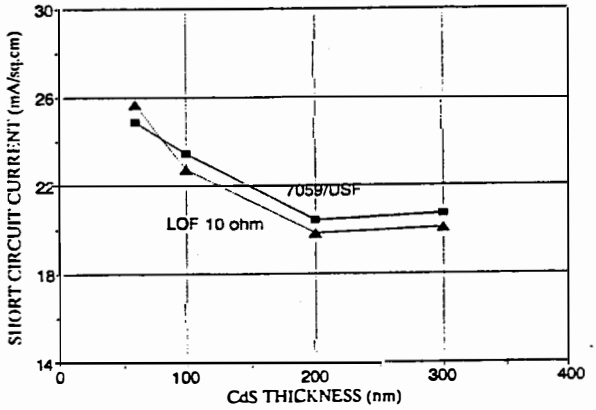

Fig. 3.9: J_{SC} for cells on 7059 and LOF glass, processed side-by-side.

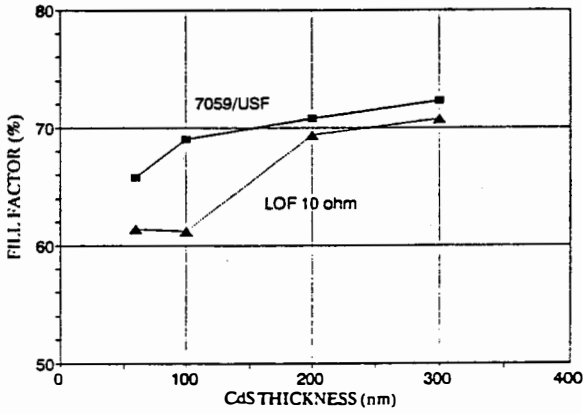

Fig. 3.10: Fill factors for 7059 and LOF cells, processed side-by-side.

3.3 Collaboration with IEC for cell contacting

In order to find a process for producing higher performing and more stable contacts for our rf sputtered cells, we collaborated with IEC for contacting. In two separate series, we used CdS/CdTe films deposited on two different LOF glass superstrates--10 Ω/□ and Tech-15 glass which has less haze and higher resistivity. The cells were prepared with a CdS thickness of 250 nm and a CdTe thickness of 1.8 μm. The process used by IEC involves 100Å sputtered copper, diffusion at 180 C in Ar, Br/methanol etch, and finally, undoped graphite. This type of contact is referred to here as

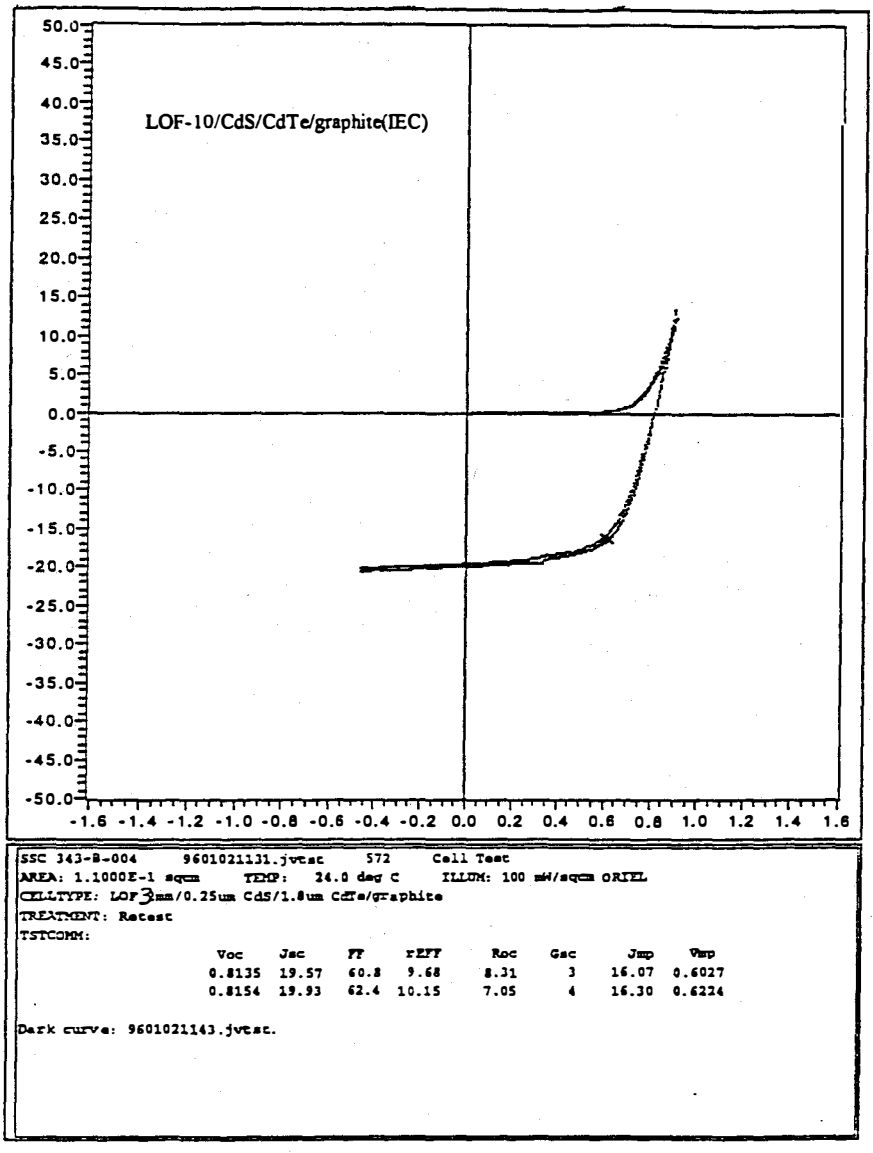

Fig. 3.11: J-V curves for IEC-contacted, rf sputtered cell on LOF SnO_2:F soda-lime glass (10Ω/□). Contact structure is 100Å/diffusion/MeOH:Br etch/graphite. Data from P. Meyers.

"method 3." Results for the method 3 contacted cells are illustrated in Figs. 3.11 and 3.12. The cell prepared on the Tech-15 glass showed about 1 mA/cm^2 better current as expected for the lower haze SnO_2 and also better fill factor. There is a remarkable difference in the forward current behavior of cells with the method-3 contacts as compared to the diffused Cu/Au. (See Fig. 3.7.) The performance of these graphite-contacted cells is stable over time in contrast to the diffused Cu/Au cells. This confirms that most of the instability with the methods-1-and-2-contacted cells is related to the contact performance. Furthermore the forward current behavior, especially in the dark, is much improved.

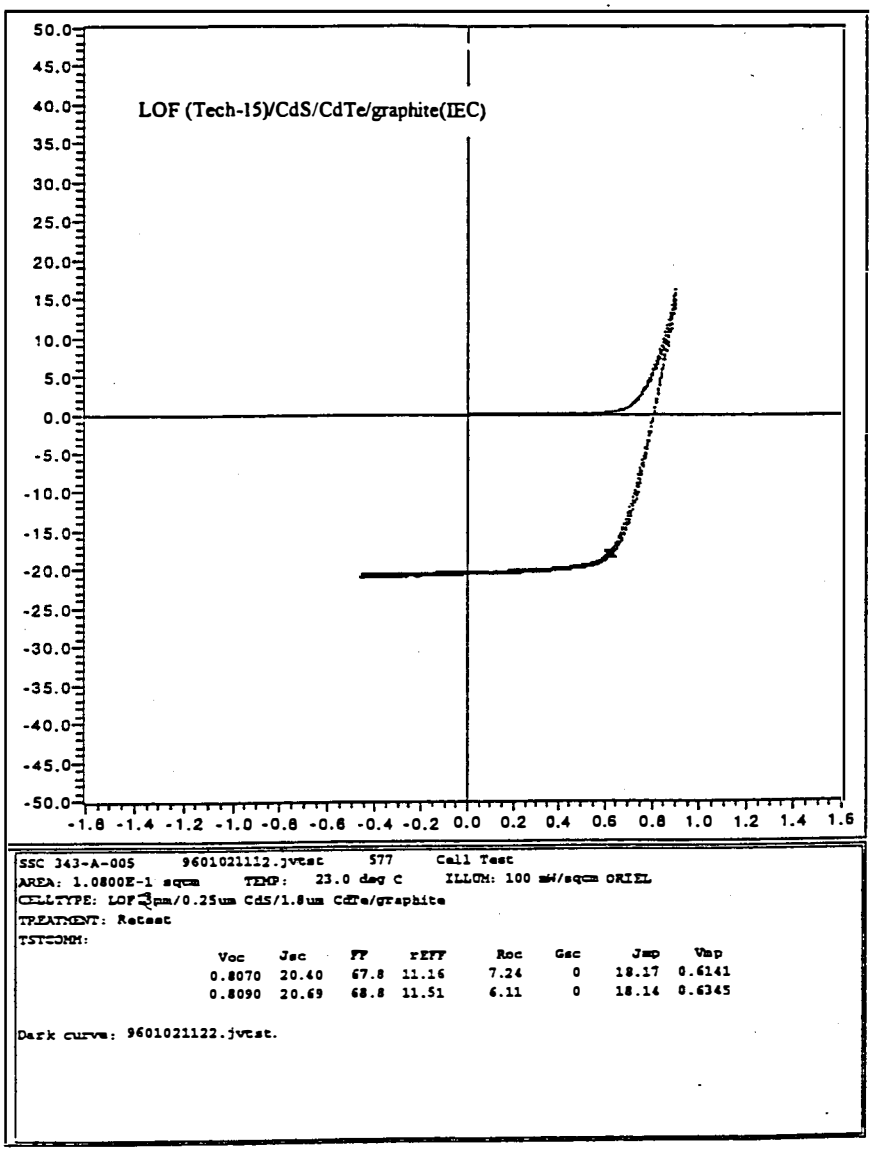

Fig. 3.12: J-V curves for IEC-contacted, rf sputtered cell on LOF Tech-15 soda-lime glass. Contact structure is 100Å/diffusion/MeOH:Br etch/graphite. Data from P. Meyers.

4.0 Studies of CdS_xTe_{1-x} alloys and CdS/CdTe interdiffusion

The heterojunction interface between CdS and CdTe is most critical to the performance of the CdS/CdTe solar cell. It is known that interdiffusion occurs during the annealing after $CdCl_2$ treatment[8,9] and possibly some interdiffusion also occurs during growth, depending on the growth temperature. It is also generally accepted that some interdiffusion is necessary for obtaining a high efficiency CdS/CdTe solar cell. Although there have been some limited studies of the nature of the ternary alloy material, CdS_xTe_{1-x}, it is relatively poorly understood. Previous studies have examined the lattice constant and optical absorption of thin films produced by co-evaporation.[10] We believe that it is important to examine the nature of these alloy films produced under conditions similar to those used in the fabrication of a solar cell.

The following two sections describe work in progress addressing the nature of these interdiffused layers. In the first study we have fabricated a wide range of the ternary alloy films by LPVD and examined their properties by optical absorption, x-ray diffraction, Raman scattering, wavelength dispersive x-ray spectroscopy (WDS), and photoluminescence. In a second study we have prepared a series of thin bilayer films of CdS/CdTe by both LPVD and rf sputtering and then examined interdiffusion by Rutherford backscattering after a series of anneals.

4.1 CdS_xTe_{1-x} film growth by laser physical vapor deposition

Although most of our present solar cell fabrication effort is focussed on rf sputtered films, we have found previously that the films produced by LPVD are very similar to those produced by rf sputtering. For example, similar superstrate temperatures are used and similar growth rates are obtained. LPVD has the advantage that we can readily prepare a series of targets from mixtures of the binary compounds, CdS and CdTe, which will yield a broad range of alloy films.[11] We fabricate these targets by cold pressing from the mixtures with a standard hand-operated press at ~10 tons/in^2.A summary of the films which have been grown to date is given in Table 4.1. The first row shows the sulfur content (average x-value) of the as-prepared targets. The second row shows the results of wavelength dispersive x-ray spectroscopy (WDS) analysis performed by Alice Mason of NREL. The third row shows the x-value of the film as inferred from the lattice constant using a linear interpolation between end-point binaries (Vegard's rule).

Table 4.1: CdS_xTe_{1-x} Films Prepared by LPVD on 7059 Glass

Sample ID	CST4	CST5	CST1	CST2	CST3	CST8	CST9	CST7	CST6	CST10
target x	0.97	0.94	0.90	0.80	0.70	0.50	0.20	0.10	0.05	0.02
film x (WDS)		0.90		0.75	0.71	0.29	0.11		0.031	
film x (x-ray)	0.99	0.93	0.92	0.85	0.77	0.27	0.11	0.03	0.018	0.006

Otical absorption in these thin films can be used to find the onset of direct band-to-band transitions and thus to infer the band gap. Band edges were obtained by extrapolation to zero of the square of the optical absorption coefficient. The inferred absorption edges are shown in Figure 4.1. The data show clearly the previously observed band bowing with a minimum occurring near x = 0.2. There is some evidence that this effect shows up in CdS/CdTe solar cells after $CdCl_2$ processing and annealing. It has the effect of shifting the red response slightly to longer wavelength. We have sent most of these alloy films to NREL for photoluminescence analysis by the group of Al-Jassim.

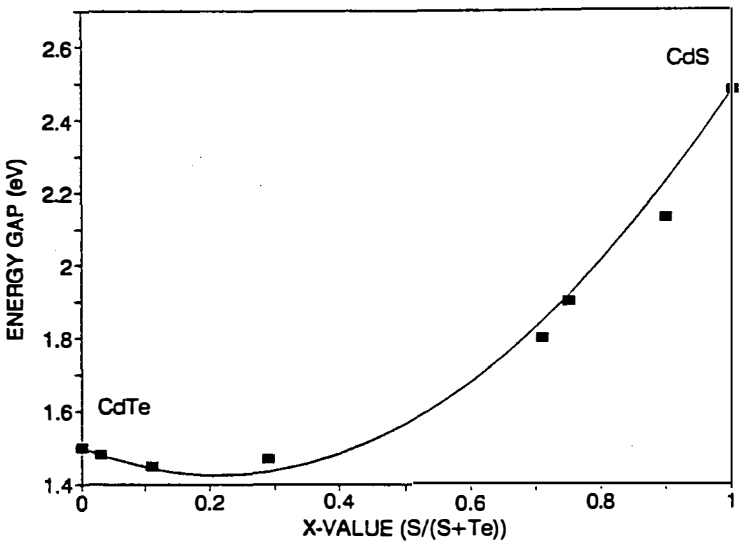

Fig. 4.1: Absorption edge vs. x-value in CdS_xTe_{1-x}.

We have done some annealing of these alloy films and have found that at intermediate x-values phase-separation occurs and the ternary alloy segregates into a Te-rich phase and a S-rich phase. When this happens, the optical absorption edge shifts and reflects the presence of the smaller bandgap phase. In addition the x-ray diffraction clearly shows the two-phase material. Preliminary Raman scattering scattering measurements also show evidence of this phase separation.

4.2 RBS measurements of CdS/CdTe interdiffusion in thin bilayers

Regions of ternary alloy material are normally produced by interdiffusion in CdS/CdTe solar cells during the post deposition annealing. In order to study this interdiffusion process, we prepared thin bilayer films for analysis by Rutherford backscattering. He^+ RBS at 2 MeV can conveniently probe CdS and CdTe layers of a total thickness of 200 to 300 nm. Because of the energy loss of the He ion as it passes through the solid, the backscattered energy of the He provides excellent depth resolution. In addition the kinematics of the backscattering process allows one to resolve elements with different masses. One limitation of the method for studying thin films is that high mass elements in the superstrate can contribute unwanted backgrounds. In fact the high Ba content of borosilicate glass causes just such problems. Therefore we chose to prepare the bilayer films on fused silica microscope slides.

Examples of the RBS spectra obtained from one such bilayer are shown in Figs. 4.2 - 4.4. The as-deposited film, Fig. 4.2, shows clearly the various layers of the film and indicates the power of the RBS analysis technique. The smooth curves are fits to the data using the RUMP[12] analysis. Fig. 4.3

shows the effect of 375 C annealing the bilayer film after LPVD $CdCl_2$ application. Fig. 4.4 shows the effect of $CdCl_2$ treatment and anneal at 400 C. The sulfur peak near channel 600 shows most clearly the effects of diffusion. As S diffuses into the CdTe (closer to the surface), the He backscatters at higher energy. The behavior is currently being modeled using the RUMP analysis.

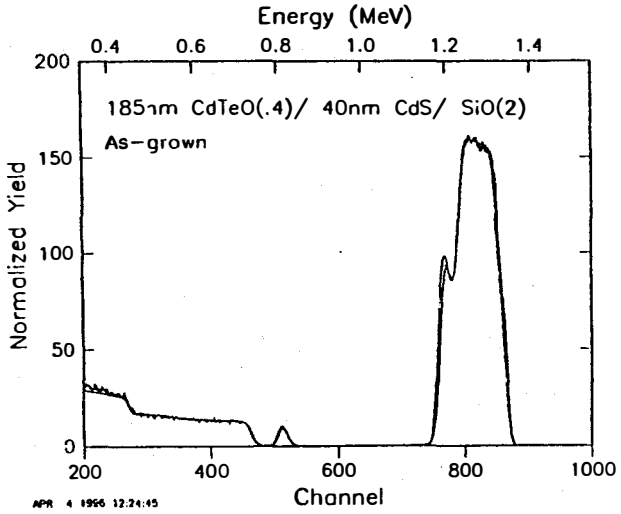

Fig. 4.2: 1.8 MeV He Rutherford backscattering spectrum of as-deposited rf sputtered bilayer--fused silica /50 nm CdS/180 nm CdTe.

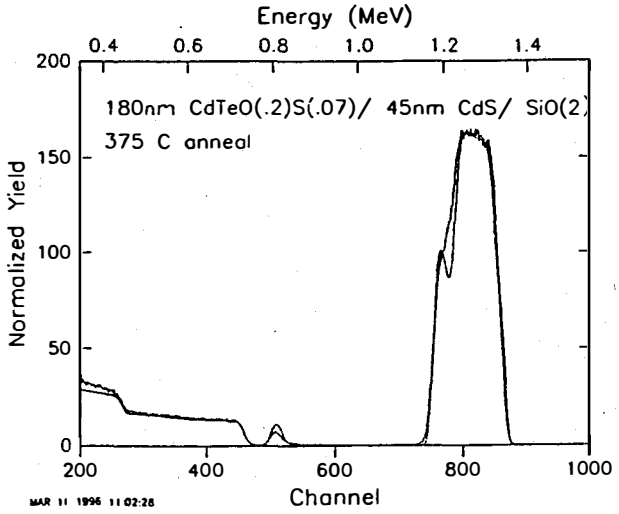

Fig. 4.3: RBS spectrum of bilayer film after $CdCl_2$ treatment and 15 min. anneal at 375 C.

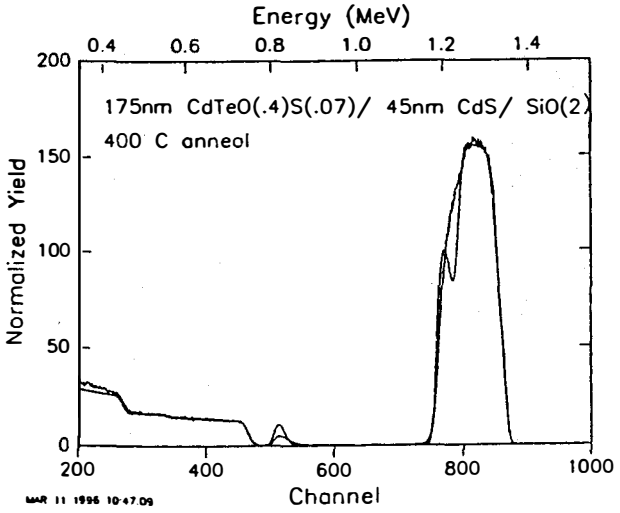

Fig. 4.4: RBS spectrum of bilayer film after $CdCl_2$ treatment and 15 min. anneal at 400 C.

5.0 Summer 1995 NSF Research Experiences for Undergraduates projects

Three undersgaduate students were involved in this photovoltaic project during the summer of 1995 as part of the National Science Foundation's Research Experiences for Undergraduates Program (REU) at the University of Toledo Department of Physics and Astronomy. The three students are David Spry, Stacy Shepard, and Mark Lenigan. David Spry was from the Univesity of Toledo who also participated last year. Stacy Shepard was from Arizona State University, and Mark Lenigan was from the University of Michigan--Dearborn. Their projects are briefly described below.

1. David Spry's project was titled "STM Measurements of surface morphology of SnO_2 with various chemo-mechanical treatments." David grew CdS films on a variety of substrates including soda-lime glass, single crystal silicon, 8, 10, & 20 Ω/□ LOF soda-lime glass, HOPG graphite, and single crystal quartz. He used a scanning tunnelling microscope to study the surface morphology of these 300 nm thick films. David also sutdied some LOF SnO_2-coated glass that had been chemo-mechanically polished in an HCl-Zn solution. This procedure produced a smoother, more uniform CdS film as determined from the frequency-height histogram obtained from the STM image. In limited tests, the chemo-mechanically polished substrates yielded cells with about 0.5 to 1% higher efficiencies.

2. Stacy Shepard's project was titled "Studies of Graphite Contacting for CdS/CdTe solar Cells." Stacy used graphite suspensions with either aqueous (Acheson Aquadag 109) or organic-based (Acheson Electrodag 114) hosts.[13] She examined the effect of etching with MeOH:Br solutions prior to the application of graphite and also the optimum curing temperature. In addition she tried the addition of dopants to the graphite suspensions. This included CuCl and HgTe mixed with the original suspensions. In the period of time available, the study was necessarily preliminary, but tentative conclusions were that the contacts were stable by yielded efficiencies about 2% lower in efficiency than our standard diffused Cu/Au contacts

3. Mark Lenigan worked on testing and designing a system for monitoring the thickness of CdS layers with an *in situ* optical monitor. For the previous 18 months we had successfully been monitoring the thickness with the 458 nm line from an Ar ion laser, using a beam relayed to our growth chamber from a laser two floors above. The set-up for each run is unnecessarily time consuming and preempted the laser for other spectroscopy work. In addition the cost of photons from the Ar ion laser is very high. Thus Mark tested out the concept of using a small Hg lamp and an optical filter. The method has limited dynamic range but is clearly feasible for monitoring CdS growth in thin layers (< 500 nm). Mark then sketched out the design for a circuit that would read the current from the light detector and feed a voltage into an analog to digital converter card in a personal computer. The circuit is presently being implemented with the use of a blue LED rather than the Hg lamp.

Although some of these summer projects were not fully completed in the 10 week summer period,

most of them have yielded significant benefits to this contract. But more important, we believe, is the benefit to the students, and we anticipate that some will pursue further work in the PV field. We have found that there are many photovoltaics-related projects which can be quite stimulating to undergraduate students.

6.0 Conclusions

During Phase Two of the present contract we continued improvement in the performance of the all-rf-sputtered CdS/CdTe cells on superstrates of LOF 10 Ω/□ soda-lime glass. The NREL-verified performance increased from the previous 10.4% to 11.6% air mass 1.5. We attribute the increase in performance partly to the use of unbalanced magnetrons for both the CdS and the CdTe layers and to some optimization of the amount of $CdCl_2$ used for the postdeposition treatment. This performance was achieved with relatively thin CdTe (1.8 μm) and without the use of any antireflection coating on the glass. Presently the performance is limited by the relatively thick CdS (250 nm) which inhibits the blue response, and by the diffused Cu/Au contacts which are not entirely stable.

Through our participation in the CdTe Thin-Film Partnership Teaming activity, we have found that the rf sputtering technique itself appears not to be fundamental limitation to further reductions in CdS thickness. Thus, the rf sputtered cells fabricated on borosilicate glass (7059) superstrates with multilayer SnO_2 coatings showed only a small drop in V_{OC} (from 0.79 V to 0.76 V) as the sputtered CdS thickness was decreased from 300 nm to 60 nm. J_{SC}, however, increased from 19.6 to 24.2 mA/cm^2 as the CdS thickness decreased. By contrast, cells on the LOF 10 Ω/□ superstrates suffered drastic losses in V_{OC} (from 0.80 to 0.49 V) when they were fabricated through all steps in the processing side-by-side with the 7059 superstrates. We believe that this indicates the importance in further work on the influence of texture and composition of the transparent conducing oxide layer(s). Additional collaborative work has focussed on the contacting issue with contact applied at the Institute for Energy Conversion. In particular contact structures with sputtered copper, diffused, etched and a final layer of graphite appear to be very stable, although in initial tests they are somewhat lower in initial efficiency.

We have continued fundamental studies of the characteristics of the rf sputtering plasma with optical emission studies and have installed a quadrupole mass spectrometer on the rf sputtering chamber in order to monitor more closely the deposition process.

Studies of the alloy CdS_xTe_{1-x} system using thin films of laser deposited material are presently nearing completion. Analysis will include band gap vs. x-value, lattice constant, phonon frequencies, and phase separation during annealing. Also we have obtained preliminary results from Rutherford backscattering analysis on thin sputtered bilayer films of CdS/CdTe on fused silica which show the progress of interdiffusion for several anneal temperatures.

7.0 Future Directions

In Phase Three of this contract we intend to place our principal effort on finding contacts with

improved stability and on a method of improving the cell response in the blue spectral region.

With respect to contacts, our tests have determined that the diffused Cu/Au contacts on the latest sputtered cell tested at NREL caused a performance deterioration by about 0.8% in absolute efficiency. Furthermore we have found encouraging results for graphite-contacted cells in collaboration with IEC. This effort will be expanded.

With respect to improved blue response, our side-by-side fabrication of cells with thin CdS on (1) soda-lime glass with standard LOF SnO_2:F and (2) on 7059 glass with TCO coating supplied by the University of South Florida show that there is no apparent fundamental limitation to the use of rf sputtering for the preparation of thin CdS layers (followed by rf sputtering for the CdTe layer). However, it appears that either the texture or the composition of the LOF SnO_2 is a limiting factor in the thin sputtered CdS. We have not, in the past, made any attempt to screen for pinholes in the CdS layer before proceeding with the CdTe deposition, since these two depositions are normally done sequentially in the same chamber without breaking the vacuum or interrupting or changing the superstrate heating. We will begin this study by quantifying the number and size of any pinholes in the rf sputtered CdS as a function of thickness.

Finally, we will complete the ongoing studies of the properties of the ternary alloy films, CdS_xTe_{1-x} and try to incorporate some of these alloys in the as-deposited films. Similarly the ongoing study of interdiffusion between CdS and CdTe using RBS techniques will be concluded to try to quantify the extent of interdiffusion as a function of anneal temperature including identifying the effect of $CdCl_2$ treatments.

8.0 Acknowledgments

Many individuals in addition to those at the University of Toledo have contributed in different ways to the work over the past year. At Solar Cells Inc., we thank Theodore Zhou, R.C. Powell and Rick Sasala for helpful suggestions as well as some contacting studies. At IEC, we are indebted to Peter Meyers and Brian McCandless for contacting studies and further suggestions.. For the CdTe Teaming activity we are indebted to Chris Ferekides of the University of South Florida for the 7059/TCO superstrates and for measurements on the completed cells to Jim Sites and Jennifer Granata of Colorado State University. For supply of superstrate material, we especially thank LOF and Peter Gerhardinger.

We are especially grateful to our contract monitor, Bolko von Roedern, for many helpful discussions and suggestions. Also at NREL we have benefitted from very helpful discussions with Pete Sheldon, Ramesh Dhere, Kannan Ramanathan, and Tim Gessert.

9.0 References

1. A.D. Compaan and R.G. Bohn, "Thin Film CdTe Photovoltaic Cells," Annual Subcontract Report, 1 Nov 1991--31 Oct 1992. [Available NTIS # NREL/TP-451-5813, DE94000201]

2. A. D. Compaan and R. G. Bohn, "Thin Film Cadmium Telluride Photovoltaic Cells," Final Subcontract Report, 1 Nov 1992--1 Jan. 94 NREL/TP-451-7162. [Available NTIS: Order No. DE9401186].

3. A. D. Compaan and R. G. Bohn, "High Efficiency Thin Film Cadmium Telluride Photovoltaic Cells," Annual Subcontract Report, 20 Jan 1994--19 Jan. 1995 NREL/TP-451-8120. [Available NTIS: Order No. DE95009256].

4. S.M Rossnagel, "Magnetron Plasma Deposition Processes," in *Handbook of Plasma Processing Technology*, edited by Rossnagel, Cuomo, and Westwood. (Noyes Publications, Park Ridge, N.J., 1990) pp. 160-182.

5. A. D. Compaan, M. Shao, C. N. Tabory, Z. Feng, A. Fischer, I. Matulionis, and R. G. Bohn, "RF Sputtered CdS/CdTe Solar Cells: Effects of Magnetic Field, RF Power, Target Morphology, and Substrate Temperature," Proc. First World Conf. on Photovoltaic Energy Conversion (24th IEEE Photovoltaic Specialists Conference) (IEEE, 1995) pp.111-114.

6. Z. Feng, C. N. Tabory, & A. D. Compaan, "*In Situ* Interference Measurements of Glass Substrate Temperature," Proc. First World Conf. on Photovoltaic Energy Conversion (24th IEEE Photovoltaic Specialists Conference), (IEEE, 1995) pp. 350-353.

7. Meilun Shao, Ph.D. Thesis, Univ. of Toledo, 1995 "CdTe and CdS Thin Film Preparation Using RF Planar Magnetron Sputtering" (unpublished)

8. I. Clemminck, M. Burgelman, M. Casteleyn, J. De Poorter, & A. Vervaet, Proc. 22nd. IEEE Photovoltaic Specialists Conf. (1991) p.1114.

9. M.E. Ozsan & D.R. Johnson, "An Analysis of Interface Structures in CdS/CdTe Solar Cells," *Proc. 12th European PVSEC* (Amsterdam, April 1994) 1995.

10. K. Ohata, J. Saraie, &T. Tanaka, Jpn. J. Appl. Phys. **12**, 1641 (1973).

11. A.D. Compaan and R.G. Bohn, "Thin Film CdTe Photovoltaic Cells," Annual Subcontract Report, July 1990--31 Oct. 1991. [Available NTIS #DE92001248]

12. Computer Graphic Service, Ltd., Ithaca, N.Y. 14850-8716.

13. Acheson Colloids Company, Port Huron, MI 48060

10.0 Publications

Refereed papers published or in press (1/95-1/96):

1. A. Fischer, A. Compaan, A. Dane and A. Aydinli, "Resonant Raman and Photoluminescence of CdTe Films for PV Using Diode Lasers," Semiconductor Processing and Characterization with Lasers--Applications in Photovoltaics [Stuttgart, Germany Apr. 18-20, 1994], Materials Science Forum, vol. 173-174, 349-354 (1995).

2. A. Compaan, M. E. Savage, U. Jayamaha, T. Azfar, and A. Aydinli, "Raman Studies of Doped Poly-Si Thin Films Prepared by Pulsed Excimer-Laser Annealing," Semiconductor Processing and Characterization with Lasers--Applications in Photovoltaics [Stuttgart, Germany Apr. 18-20, 1994], Materials Science Forum, vol. 173-174, 197-202 (1995).

3. J.J. Dubowski, A. Compaan, M. Prasad, "Laser-Assisted Dry Etching Ablation of InP," European Mat. Res. Soc. Meeting Strasbourg, France, May 24-27, 1994 (Symposium B: Photon-Assisted Processing of Surfaces and Thin Films.), Appl. Surf. Sci. **86**, 548-553 (1995).

4. A. Compaan, "Infrared," "Raman Scattering," and "Solar (Photovoltaic) Cells." three short articles for the Macmillan Encyclopedia of Physics, J.S. Rigden, editor-in-chief. (in press, 1996)

5. A.D. Compaan, M. Shao, C.N. Tabory, Z. Feng, A. Fischer, I. Matulionis, and R.G. Bohn, "RF Sputtered CdS/CdTe Solar Cells: Effects of Magnetic Field, RF Power, Gas, Pressure, and Substrate Temperature," (First World Conference on Photovoltaic Energy Conversion, Hawaii Dec. 5-9, 1994), Proc. 24th IEEE Photovoltaic Specialists Conference 1994, pp. 111-114 (1995).

6. Z. Feng, C.N. Tabory, and A.D. Compaan, "*In Situ* Measurements of Glass Substrate Temperatures," (First World Conference on Photovoltaic Energy Conversion, Hawaii Dec. 5-9, 1994), Proc. 24th IEEE Photovoltaic Specialists Conference 1994, pp. 350-353 (1995).

7. R.G. Bohn, C.N. Tabory, C.Deak, M. Shao, A.D. Compaan, and N. Reiter, "RF Sputtered Films of Cu-Doped and N-Doped ZnTe," (First World Conference on Photovoltaic Energy Conversion, Hawaii Dec. 5-9, 1994), Proc. 24th IEEE Photovoltaic Specialists Conference 1994, pp. 354-356 (1995).

8. A. Compaan, "Laser Processing of Thin Film Photovoltaics," Laser-Induced Thin Film Processing, edited by J. J. Dubowski (SPIE Proceeding vol. 2403, SPIE, Bellingham, WA 1995).

9. A. Compaan, M. Pearce, P.M. Voyles, D. Spry, Z. Feng, A. Fischer, M. Shao, & R.G. Bohn,

"Pulsed Laser Deposition for CdTe-based Photovoltaics," in Laser-Induced Thin Film Processing, edited by J.J. Dubowski, Proc. of the SPIE, vol 2403, pp. 232-239 (SPIE, Bellingham, WA, 1995).

10. A. D. Compaan, M. Shao, C. N. Tabory, Z. Feng, A. Fischer, F. Shan, C. Narayanswamy and R. G. Bohn, "Magnetic Field Effects in RF Magnetron Sputtering of CdS/CdTe Solar Cells," 13th NREL PV Program Review," edited by H.S. Ullal and C.E. Witt, (AIP Conference Proceedings #353, 1995) pp. 360-367.

Annual Subcontract Report:

1. A. D. Compaan and R. G. Bohn, "High Efficiency Thin Film Cadmium Telluride Photovoltaic Cells," Annual Subcontract Report, 20 Jan 1994--19 Jan. 1995 NREL/TP-451-8120. [Available NTIS: Order No. DE95009256].

Annual Reports published in NREL Annual Report, PV Subcontract Program:

1. A.D. Compaan, R.G. Bohn, Y. Rajakarunanayake, C.N. Tabory, M. Shao, A. Fischer, Z. Feng, F. Shen, C. Narayanswami, and I. Matulionis, "High Efficiency Thin Film Cadmium Telluride Photovoltaic Cells," NREL Photovoltaic Program FY 1994 Annual Report. (Available NTIS report no. NREL/TP-410-7993, DE95009244.)

2. A.D. Compaan, R.G. Bohn, G. Contreras-Puente, C.N. Tabory, M. Shao, U. Jayamaha, A. Fischer, Z. Feng, C. Narayanswami, and D. Grecu, "High Efficiency Thin Film Cadmium Telluride Photovoltaic Cells," NREL Photovoltaic Program FY 1995 Annual Report (to be published).

11.0 Visiting Faculty, Students, and Research Assistants Participating in the Project

Visiting faculty member:

Gerardo Contreras-Puente has participated in this project with University of Toledo support from September 1995 while on sabbatical leave from the Polytechnic Institute in Mexico City.

Students:

Meilun Shao
Ph.D. June 1995 "CdTe and CdS Thin Film Preparation using RF Planar Magnetron Sputtering"

Andreas Fischer
Ph.D. in progress

Zhirong Feng
Ph.D. in progress

Faming Shen
M.S. June 1995 "Capacitance-Voltage Measurements on CdS/CdTe Solar Cells"

Chitra Narayanswamy
M.S. in progress

Dan Grecu
Ph.D. in progress

Technical Assistant: (1/95--8/95)

Charles N. Tabory (deceased)

Postdoctoral Associate: (9/95--)

Upali Jayamaha

REPORT DOCUMENTATION PAGE

Form Approved
OMB NO. 0704-0188

1. AGENCY USE ONLY (Leave blank)	2. REPORT DATE	3. REPORT TYPE AND DATES COVERED
	May 1996	Annual Technical Report, 20 January 1995 - 19 January 1996

4. TITLE AND SUBTITLE

High-Efficiency Thin-Film Cadmium Telluride Photovoltaic Cells

5. FUNDING NUMBERS

C: ZAX-4-14013-1

TA: PV631101

6. AUTHOR(S)

A.D. Compaan, R.G. Bohn, and G. Contreras-Puente

7. PERFORMING ORGANIZATION NAME(S) AND ADDRESS(ES)

Department of Physics and Astronomy
University of Toledo
Toledo, Ohio 43606

8. PERFORMING ORGANIZATION REPORT NUMBER

9. SPONSORING/MONITORING AGENCY NAME(S) AND ADDRESS(ES)

National Renewable Energy Laboratory
1617 Cole Blvd.
Golden, CO 80401-3393

10. SPONSORING/MONITORING AGENCY REPORT NUMBER

TP-451-21233

DE96007892

11. SUPPLEMENTARY NOTES

NREL Technical Monitor: B. von Roedern

12a. DISTRIBUTION/AVAILABILITY STATEMENT

12b. DISTRIBUTION CODE

UC-1260

13. ABSTRACT *(Maximum 200 words)*

This annual report covers the second year of a 3-year NREL subcontract with the University of Toledo that is focused on improvements in efficiency for radio frequency (rf)-sputtered CdS/CdTe solar cells. In earlier work supported by NREL, the University of Toledo established the viability of two new deposition methods for CdS/CdTe solar cells by fabricating cells with efficiencies greater than 10% at air mass (AM) 1.5 on soda lime glass for "all-sputtered" cells and also for "all-laser-deposited" cells. Most of our effort has been placed on radio frequency sputtering (RFS) because it was judged to be more economical and more easily scaled to large-area deposition. However, laser physical vapor deposition (LPVD) has remained our method of choice for the deposition of $CdCl_2$ layers and also for the exploration of new materials such as the ternary alloys including CdS_xTe_{1-x} and dopants such as Cu in ZnTe.

14. SUBJECT TERMS

photovoltaics ; solar cells ; high efficiency ; cadmium telluride ; deposition

15. NUMBER OF PAGES
38

16. PRICE CODE

17. SECURITY CLASSIFICATION OF REPORT	18. SECURITY CLASSIFICATION OF THIS PAGE	19. SECURITY CLASSIFICATION OF ABSTRACT	20. LIMITATION OF ABSTRACT
Unclassified	Unclassified	Unclassified	UL